Environmental Science
Advances

CRITICAL REVIEW

View Article Online
View Journal | View Issue

Check for updates

Cite this: *Environ. Sci.: Adv.*, 2023, **2**, 1167

Integrated 3D pore architecture design of bio-based engineered catalysts and adsorbents: preparation, chemical doping, and environmental applications†

Dinh Viet Cuong,[a] Jhen-Cih Wu,[b] Eakalak Khan, [c] Gijs Du Laing, [d]
Yong Sik Ok *[ef] and Chia-Hung Hou *[bg]

An integrated strategy combining 3D architecture design and chemical doping holds great promise for enhancing the performance of bio-based engineered carbon materials in environmental applications. This review paper critically examines the use of integrated hierarchical porous carbon derived from biomass (bio-based IHPC) as an engineered catalyst and adsorbent for environmental purposes. The hierarchically interconnected pore architectures can reduce the electrical resistance and shorten the diffusion pathway, which is beneficial for the transport of ions/molecules. Additionally, the high pore volume, large specific surface area, and abundant active sites contribute to the high capacity for ion and molecule capture. The bio-based IHPC with 3D interconnected hierarchical porous structures can be obtained through non-templating, hard-templating and self-templating strategies. Chemical doping can further create functional groups and active sites on the bio-based IHPC surface, resulting in an abundance of reaction and interaction with pollutants. In particular, the surface properties of bio-based IHPCs can be further modified by heteroatom doping or metal (hydr)oxide coating. The review demonstrates the efficiency of bio-based IHPC as an engineered catalyst and adsorbent in various environmental applications. These applications include the removal of toxic trace elements and organic pollutants, carbon capture, enhancement of anaerobic digestion processes, antimicrobial treatment, and oil–water separation. The paper thoroughly discusses the influence mechanisms of pore architectures and chemical doping on the performance of bio-based IHPC in these applications. Finally, the paper concludes by presenting promising research directions for the preparation and application of bio-based IHPC.

Received 8th May 2023
Accepted 16th July 2023

DOI: 10.1039/d3va00125c

rsc.li/esadvances

Environmental significance

The rapid urbanization and industrialization of cities around the world have resulted in severe environmental pollution caused by a range of pollutants including heavy metals, organic matter, and greenhouse gases. This study aims to address these environmental challenges by critically reviewing the potential of integrated 3D pore architecture design in bio-based engineered catalysts and adsorbents. By combining chemical doping with 3D architectural design, the performance of biomaterials can be significantly enhanced for addressing environmental pollution. This approach holds great potential for environmental remediation, particularly in developing countries where biomass is abundant yet underutilized and environmental treatment facilities are often inadequate. Our proposed methods and findings have important implications for promoting sustainable development globally, and we hope that they will inspire future research in this field.

1. Introduction

A porous carbon material, developed by integrating 3D architecture design and chemical doping, referred to as integrated hierarchical porous carbon (IHPC), has been recently recognized as a high potential material for efficient water and wastewater treatment and carbon capture.[1–5] Notably, many attempts have been made with a focus on integration strategies

---

[a] *Faculty of Environmental Engineering, Hanoi University of Civil Engineering, Hanoi 100000, Vietnam*

[b] *Graduate Institute of Environmental Engineering, National Taiwan University, Taipei 10617, Taiwan. E-mail: chiahunghou@ntu.edu.tw*

[c] *Civil and Environmental Engineering and Construction Department, University of Nevada, Las Vegas, NV, USA*

[d] *Department of Green Chemistry and Technology, Ghent University, Ghent, Belgium*

[e] *Korea Biochar Research Center, APRU Sustainable Waste Management & Division of Environmental Science and Ecological Engineering, Korea University, Seoul, 02841, Republic of Korea. E-mail: yongsikok@korea.ac.kr*

[f] *International ESG Association (IESGA), Seoul, 06621, Republic of Korea*

[g] *Research Center for Future Earth, National Taiwan University, No. 1, Sec. 4. Roosevelt Rd., Taipei 10617, Taiwan*

† Electronic supplementary information (ESI) available. See DOI: **https://doi.org/10.1039/d3va00125c**

of pore architecture and surface chemistry to achieve superior performance for pollutant removal. Unlike traditional porous carbon materials, the designed pore architecture in IHPC is a unique 3D interconnected hierarchical porous structure in terms of micropores (<2 nm), mesopores (2–50 nm), and macropores (>50 nm) (Fig. S1†).[6] The size, distribution and component ratio of macropores, mesopores and micropores in IHPCs can be well controlled through the preparation process (*e.g.*, carbonization, leaching, and activation) by changing various factors (*e.g.*, activation agent, temperature and time). This 3D interconnected hierarchical porous structure has the potential to significantly improve pollutant removal efficiency. Specifically, macropores play the role of buffering reservoirs to minimize the transport distance into the pore channels during diffusion. The presence of mesopore channels inside the IHPC structure can reduce the mass transfer resistance of ions and molecules, leading to faster transport to micropores and providing a large accessible surface area for adsorption.[7] Micropores generate an abundant number of active sites that are helpful for enhancing ion and molecule adsorption.[8,9]

On the other hand, the involvement of surface chemistry and chemical doping, such as surface functional groups and coated metal compounds (Fig. S1†), can offer a variety of interactions/reactions for surface-related processes, *e.g.*, adsorption and redox transformation.[10–12] Therefore, chemical doping is considered to be an encouraging step to diversify the surface chemistry ingredients of IHPC for pollutant treatment efficiency. O doping is one of the most common chemical surface modifications of carbon materials. O functional groups can be produced from natural and synthetic precursors or O-containing activation agents (CO_2, NaOH, KOH, K_2CO_3, or H_2O). O functional groups on IHPC include acidic groups (*e.g.*, carboxyl, phenol, lactol and lactone) and basic groups (*e.g.*, chromene, pyrone, and diketone/quinone structures).[12] N-doped carbon materials have also been widely used to enhance performance in environmental applications.[13–15] N functionalities, including pyrrolic/pyridone, pyridinic, quaternary N, and pyridine-N-oxide, may be observed on IHPC.[13,16] Unlike O functionalities, N functionalities are not prevalent on the carbon matrix of IHPC. Doping N on IHPC is usually performed by using N-enriched biomass or inserting N atoms into the carbon surface, *e.g.*, post-treatment with ammonia gas or employing a N-containing precursor.

Among a variety of precursors (*e.g.*, organic matter and fossil fuels) for preparing IHPC, biomass is a promising precursor for the production of carbon materials for managing waste streams. The unique characteristics of biomass include being environmentally sustainable, naturally renewable, affordable, abundant and easily accessible.[17–19] The development of bio-based materials provides great opportunities for sustainable environmental applications. This is because IHPC not only has the potential to replace conventional carbon materials (*e.g.*, activated carbon) but also contributes to effective solid waste management by reducing the emissions to the environment. In the circular economy concept, the utilization of biomass as feedstock can maximize creative value and minimize environmental impact.[20,21]

Recent studies have demonstrated the feasibility of using bio-based IHPCs for the removal of heavy metals[22] and organic pollutants,[23] carbon capture,[24] and enhancing anaerobic digestion (AD) processes,[25] antimicrobial treatment,[5] and oil–water separation.[26] Bio-based IHPCs have also been used for desalination or water softening based on the electrosorption mechanism,[27,28] supercapacitors and the hydrogen evolution reaction.[29–31] However, the majority of previous review papers focused solely on the role of hierarchical porous structures in traditional HPC without chemical doping. This paper provides a comprehensive review on the fabrication (*i.e.*, pore structure design and chemical doping methods), environmental applications and pollutant removal mechanisms of bio-based IHPCs. The simultaneous influence of pore architecture design and chemical doping on pollutant removal efficiency has not been adequately investigated. The focus of this review is on the preparation and applications of bio-based IHPC materials in environmental remediation. Two distinctly applicable approaches are discussed for utilizing bio-based IHPCs in environmental remediation: (1) employing them as catalysts (Section 3) and (2) utilizing their adsorption capabilities (Sections 4 and 5). Additionally, the environmental applications of bio-based IHPC are discussed for enhancing anaerobic digestion processes, antimicrobial treatment, and oil–water separation (Section 6). Notably, insights into the mechanisms of inorganic (or metal(loid)s or potentially toxic elements), organic pollutant removal and carbon capture by the contributions of both the hierarchical pore architecture and chemical doping in bio-based IHPCs are critically discussed. Finally, future research perspectives are also offered.

2. Integration strategies for bio-based IHPC

2.1. Pore architecture design of IHPC

Non-templating strategy. Bio-based IHPCs can be typically fabricated by a non-templating method (Fig. 1a and b). In the non-templating method, the preparation of bio-based IHPCs can be performed by one-step carbonization,[22,32] two-step carbonization,[33] one step of carbonization and activation,[22] one-step activation[34–37] and two steps of carbonization and activation[38–40] (Table S1†). One-step and two-step carbonization are known as the eco-friendliest approaches to synthesize IHPC from biomass. In addition, the physical activation process using CO_2, steam, and air is cost-effective. However, these procedures may have difficulty in tailoring the formation of the hierarchical pore architecture with desired pore characteristics, morphology and pore size distribution. On the other hand, the two-step strategy of chemical activation and carbonization is more complex and less environmentally friendly, but the porosity can be easier to manipulate leading to a high specific surface area (SSA) and larger pore volume (PV).

Hard-templating strategy. To control the development of a 3D pore structure, a templating method can be used. Two common strategies are soft templating (using amphiphilic block copolymers as structure-directing agents) and hard

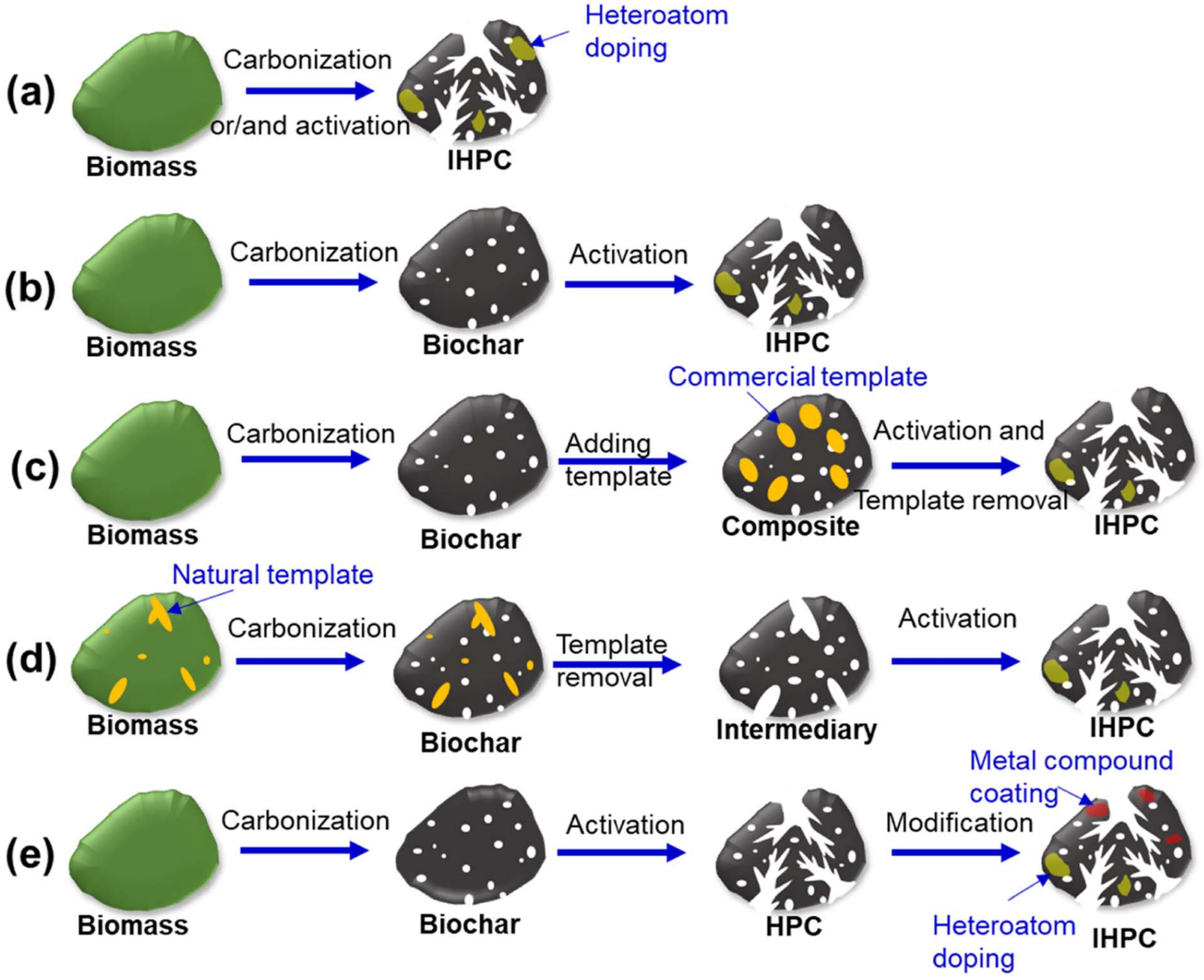

Fig. 1 Preparation of IHPC through different strategies of (a) non-templating with one step,[22,37] (b) non-templating with multiple steps,[124,142] (c) hard templating,[43,45] (d) self-templating,[23,48] and (e) chemical surface modification.[63,77]

templating (using solid-state inorganic matter as a frame structure).[41] In the preparation of bio-based IHPC, commercial hard templates, *e.g.*, Ni particles,[42] $CaCO_3$,[43,44] $ZnCl_2$ and $Mg_5(OH)_2(CO_3)_4$,[45] have been employed (Table S1†). As seen in Fig. 1c, the preparation of bio-based IHPC using the hard-templating method may include the following steps: (1) biomass carbonization to produce biochar; (2) addition of a commercial template and (3) activation to construct the hierarchical porous structure; (4) acid washing to remove the templates. However, the disadvantage of bio-based IHPC synthesis by the hard-templating method is the requirement of synthesized or attached inorganic matter as a hard template, which is complex and expensive.[6] Additionally, template removal by using acid or base solutions is usually highly corrosive and environmentally unfriendly.

Self-templating strategy. Naturally available templates can be obtained from biomass such as $CaCO_3$ in soft pitch,[46] metal–organic frameworks (MOFs) in *Enteromorpha prolifera*[47] and SiO_2 in rice husk.[48–50] The self-templating method refers to the process of producing bio-based IHPCs using these natural templates (Fig. 1d). Some major steps can be included, that is, carbonization, template leaching and activation.[1] The leaching steps can be performed by using an acid (*e.g.*, HCl, HF, or NH_4HF_2) or a base (*e.g.*, NaOH) to remove these natural templates. Notably, the high mesoporosity is beneficial for ion and pollutant transport inside bio-based IHPCs.[51,52] As shown in Table S1,† bio-based IHPC, which was prepared by the self-templating method, exhibited a high mesoporosity fraction from 55.5 to 81.1%. A major reason for the high mesoporosity achieved is the extraction of the natural template by acid or base leaching steps.

2.2. Chemical doping on bio-based IHPC

Another promising solution for manufacturing bio-based IHPC is to pre-fabricate hierarchical porous carbon (HPC) from bio-based precursors with a hierarchical porous structure but lacking robust surface functional groups. To improve the surface activity of HPC, bio-based IHPC can be further treated by a chemical doping process (Fig. 1e). The improved chemical properties can provide more reaction sites for surface-related processes between target compounds and bio-based IHPC surfaces. Bio-based IHPCs can be modified to attain desirable chemical properties by loading metals, metal oxides and hydroxides. Heteroatom (O, N, P, B, *etc.*) doping can be conducted to improve surface chemistry. N-doped bio-based IHPC was developed by incorporating N into carbon frameworks *via* N-enriched biomass.[53] N-doped IHPC derived from algae was prepared for gas-mixture separation.[54] Poplar catkins contain many amino acids as natural N sources to prepare N-doped IHPCs for CO_2 capture.[55] N,P-co-doped IHPC derived from oil-tea shells was synthesized by a combination of H_3PO_4 activation and amino (polyethyleneimine, PEI) modification.[56] Soybean cakes can be used to develop heteroatom-doped IHPC because their endosperm is rich in O, N, and P.[22] Shrimp shells, as an eco-friendly, renewable and abundant source, were successfully converted into N-doped IHPCs.[57] Silkworm cocoons, as natural biomass with high N and O contents, are beneficial for preparing O- and N-doped IHPC.[58]

N-doped IHPC can be produced by employing an N-containing precursor (such as melamine, urea, and hexamethylenetetramine) or post-treatment with ammonia gas.[59] The 3D interconnected structure of the IHPC was examined through several techniques, including N_2 adsorption–desorption isotherm analysis (Fig. S2a†), scanning electron microscopy (SEM), and transmission electron microscopy (TEM) analysis (Fig. S2b†). Additionally, the X-ray photoelectron spectroscopy (XPS) results of the N/O-doped palm sheath-based IHPC are presented in Fig. S2c.†[60] Different ratios of N contents with tailored porosity properties of the IHPC materials were controlled by the change in palm sheath biochar/activation agent ($NaNH_2$) masses (*i.e.*, 1/1, 1/2, and 1/3). Pyrrole, pyridone and pyridine functional groups were introduced on the surface of the IHPC (Fig. S2d†).

Biobased IHPCs can be modified with desirable chemical properties by loading metals, metal oxides and hydroxides. The existence of the 3D interconnected structure (Fig. S3a†) can be confirmed using SEM and TEM analyses. Furthermore, the successful coating of FeOOH on bamboo-based IHPC to remove As(III) is supported by changes observed in X-ray diffraction analysis (XRD) (Fig. S3b†), Raman spectroscopy (Fig. S3c†), and XPS analysis (Fig. S3d†).[61] Notably, ultrathin FeOOH nanosheets provided a large SSA and abundant active sites, while the hierarchically porous structure facilitated fast mass transport during the adsorption process.[61] Introducing Fe_3O_4 nanoparticles on bio-based IHPCs was conducted by Zhou *et al.*[62] These particles can be conveniently separated from the liquid phase with the assistance of an applied magnetic field. Zhou *et al.* synthesized IHPC/MgO composites for acetone adsorption.[63] The combination of highly active MgO nanoparticles and 3D pore architecture was discovered to be an important factor in acetone adsorption.

3. Bio-based IHPC as a promising catalyst for water and wastewater treatment

Catalysis is of great importance and has been widely applied in many fields of science. For water and wastewater treatment, several catalytic-related processes have been used, such as photocatalysis, sulfate radical-based advanced oxidation processes (SR-AOPs) and electrochemical advanced oxidation processes (EAOPs). The basis of these processes depends on the reactions at the interface of catalysts and reactants (*e.g.*, pollutants, persulfate (PS) and peroxymonosulfate (PMS)), and/or the formation of reactive active species (*e.g.*, hydroxyl radicals ($^\bullet$OH), sulfate radicals ($SO_4^{\bullet-}$) and superoxide anion radicals ($O_2^{\bullet-}$)) in the bulk liquid. Therefore, for the design of catalysts, it is critical to boost catalytic performance and facilitate chemical transformations.

Noble metals or metal oxides, such as Pt, IrO_2 and RuO_2, have been demonstrated to be effective catalysts; however, the high cost, scarcity and poor durability of metallic catalysts limit their field-scale applications.[64,65] Additionally, in the field of photocatalysis, metal oxides or metal sulfide catalysts, such as TiO_2, ZnO, CdS and MnO_2, also suffer from relatively low stability toward photocorrosion, a wide bandgap and a lack of light absorption in the visible light region.[66] From a practical point of view, developing alternative efficient, low-cost and stable catalysts has been eagerly anticipated in recent years.

Bio-based carbon materials with a specially designed integration architecture have gained much attention as metal-free catalysts because of their outstanding properties, *e.g.*, special surface functional groups, tunable specific surface area, low cost, natural abundance, high catalytic activity and environmentally friendly characteristics. These desirable properties can significantly enhance the performance and ensure the sustainability of catalytic processes. Several strategies for surface functionalization of bio-based IHPC catalysts can be applied, such as (1) heteroatom (*e.g.*, N, P, F, S, and O) doping, (2) introduction of metal carbides or metal sulfides (such as Ni_xC, Fe_xC, Co_xC or MoS_2), (3) incorporation of transition metal oxides (*e.g.*, CoO, Co_3O_4, MnO_2, Fe_3O_4, $MnFe_2O_4$ and $CoFe_2O_4$), (4) semiconductor (*e.g.*, TiO_2) heterojunctions, and (5) other chemical doping. This section will focus on the potential of bio-based IHPCs applied in catalytic-related processes for water and wastewater treatment.

3.1. IHPC-supported photocatalysis process

Photocatalysis has been widely investigated as a promising water treatment process by generating active species (*i.e.*, photoelectrons (e^-), photoholes (h^+), superoxide anion radicals ($O_2^{\bullet-}$), hydroxyl radicals ($^\bullet$OH), *etc.*) to degrade pollutants in water and wastewater.[67] Recently, substantial efforts have been devoted to preparing heterojunction photocatalysts, especially modifying semiconductors with carbon-based materials, as depicted in Fig. 2a. Among various carbon-based materials, bio-based IHPCs with a 3D porous structure have been viewed as profitable support candidates for the development of sustainable processes in water and wastewater treatment[68–70] (Table 1). For example, Shi *et al.* utilized a winter melon-derived carbonaceous aerogel (CA) as a support to synthesize a novel binary TiO_2/CA composite. Benefiting from the unique 3D interconnected network porous structure of CA, the TiO_2/CA composites provided efficient separation of electron–hole pairs and further reduced TiO_2 photocorrosion. The TiO_2/CA system photocatalyst demonstrated good efficacy in the photocatalytic degradation of organic pollutants, achieving an efficiency of 82% for methylene blue and

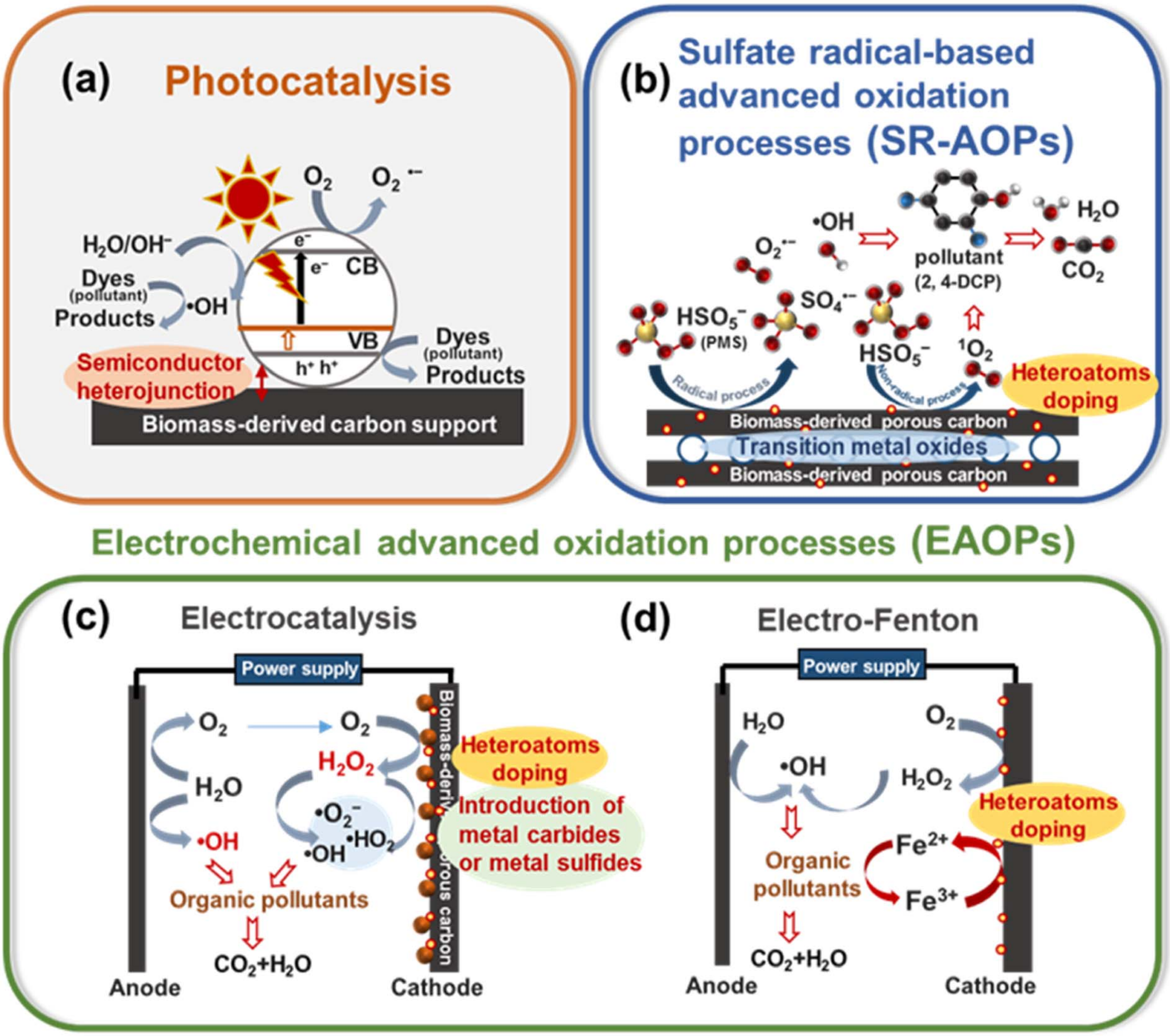

Fig. 2 Working mechanisms of (a) photocatalysis, (b) sulfate radical-based advanced oxidation processes, (c) electrocatalysis and (d) electro-Fenton *via* bio-based IHPC catalysts. Information regarding the aforementioned mechanisms was adopted from ref. 13, 73, 76, 86 and 90.

65% for ciprofloxacin, indicating the effective reliability of this approach for water decontamination.[71]

Notably, according to previous reports, the combination of bio-based IHPC with semiconductors might cause the narrowing of band gaps and enhance the adsorption capacity of photocatalysts.[72,73] Additionally, a bio-based support, acting as an electron reservoir, can further promote electron transfer from TiO_2 to carbons, avoiding the recombination of e^-/h^+ pairs.[74] The mechanism is depicted schematically in Fig. 3a. Heteroatoms from natural biowaste doping in TiO_2 lattices can also strengthen the photodegradation activity by narrowing the bandgap of photocatalysts and effectively retarding recombination of electron–hole pairs. As reported, Zhou *et al.* reported that N-doped magnetic three-dimensional carbon microspheres@TiO_2 (N-doped MCMs@TiO_2) presents greatly enhanced photocatalytic activity under visible light illumination compared with pure photocatalysts due to the N-doped carbon structure. As shown in Fig. 3b, the prepared N-doped MCMs@TiO_2 obtains good degradation performance (83.80% for methyl orange and 74.37% for tetracycline) and exhibits remarkable stability (evidenced by 85.86% after five consecutive runs) for sustainable removal of organic pollutants (*i.e.*, methyl orange) from water.[75]

3.2. IHPC-assisted sulfate radical-based advanced oxidation processes (SR-AOPs)

Sulfate radicals ($SO_4^{\bullet-}$) produced from persulfate (PS) and peroxymonosulfate (PMS) activation processes are recognized as highly reactive oxidants for degrading pollutants in water and wastewater. Most commonly, carbon-based materials have been reported to be efficient catalysts for activating PS and PMS. Moreover, the incorporation of transition ions and heteroatom doping can further enhance the catalytic activity of carbon-based materials.[76–78] The mechanism is depicted in Fig. 2b, including radical and nonradical processes. Among all candidates, N doping is the most commonly used method to tailor the catalytic properties of carbon *via* (1) creating an effective defect site by replacing a carbon atom, (2) activating

Table 1 Application of bio-based IHPC catalysts for water and wastewater treatment

Catalyst	S_{BET} ($m^2\ g^{-1}$)	Catalyst dose (mg L^{-1}) (gap band (eV))	Concentration of pollutant	Degradation efficiency (%)	Reaction time (min)	Ref.
Photocatalysis process						
TiO_2/winter melon-based IHPC	113	250/(—)	40 mg L^{-1} methylene blue	82	210	71
MOF/corncob-based IHPC	2944	50/(2.7)	20 mg L^{-1} rhodamine B	100	75	69
		100/(2.7)	50 mg L^{-1} tetracycline	98	120	
$LaMnO_3$/N-doped soybean dreg-based IHPC	129	400/(2.2)	20 mg L^{-1} direct green BE	96	180	70
Pomelo peel and melamine-based IHPC	190	250/(2.4)	20 mg L^{-1} rhodamine B	97	120	66
TiO_2/plane tree fluff-based IHPC	386	187.5/(2.7)	~16 mg L^{-1} methylene blue	100	15	13
Sulfate radical-based advanced oxidation processes						
Nickel embedded in N-doped waste-based IHPC	558	50	20 mg L^{-1} orange II	98	120	81
N-doped wheat flour-based IHPC	1791	26	0.04 mM losartan potassium	100	240	76
$MnFe_2O_4$/corn straw-based IHPC	389	50	20 mg L^{-1} orange II	100	6	77
CoO/N-doped biomass Schiff-based IHPC	454	300	50 mg L^{-1} 4-chlorophenol	100	30	78
N, S-doped human hair-based IHPC	2430	80	25 mg L^{-1} bisphenol A	98	60	82
Electrochemical advanced oxidation processes						
Tea leaf-based IHPC cathode	1620	—	100 mg L^{-1} phenol	95	120	89
MoS_2/O and N-doped cornstalk-based IHPC cathode	114	—	100 mg L^{-1} phenol	97	120	90
F-doped *Scindapsus aureus*-based IHPC cathode	531	—	Secondary effluent of refinery wastewater (TOC 22.9 mg L^{-1})	56	60	93
N- and O-doped black soybean-based IHPC cathode	664	—	50 mg L^{-1} chloramphenicol	100	80	73
Pyrrolic N-doped biomass-derived IHPC cathode	2166	—	50 mM bromocresol green	96	105	87
Taraxacum mongolicum-based IHPC cathode	799	—	Methylene blue	96	94	88

the π electrons of sp^2 carbon by N bonding configuration and (3) modifying the electron density of carbon atoms adjacent to N atoms.[79,80] For example, Ni embedded in N-doped CNTs supported on bio-based IHPC exhibited superior catalytic activities toward both organic pollutant degradation and metal reduction. The results showed that nearly 100% degradation of dye-based chemicals was achieved.

Rationally designed architectures, such as embedded Ni^0 nanoparticles, additional doping of N, hierarchical porous structures and interconnected CNTs, can provide abundant active sites and promote electron transfer, offering exciting opportunities for practical applications (Fig. 3c).[81] Similarly, an excellent degradation of 98.4% was achieved by human hair-based N,S-doped IHPC pyrolyzed at 800 °C. The results indicated that N doping (*e.g.*, graphitic N) and thiophene sulfur (*e.g.*, –C–S–C bonds) can adjust the electron density of adjacent carbon atoms and then activate PMS *via* peroxide O–O bond cleavage resulting in the production of $SO_4^{\bullet-}$ and $^{\bullet}OH$ responsible for the degradation of organic pollutants. On the other hand, PMS can also be activated by sp^2-hybridized carbon structures, in which HSO_5^- will decompose and then produce $^1O_2$ to degrade bisphenol A (BPA) (Fig. 3d).[82] Furthermore, the incorporation of transition metal oxides, such as Fe_3O_4 and $CoFe_2O_4$, in the catalysts can also efficiently activate PMS or PS for the degradation of pollutants (*i.e.*, 4-chlorophenol and bisphenol A) because of their high catalytic activity.[83,84]

3.3. IHPC-assisted electrochemical advanced oxidation processes

Electrocatalysis. Electrocatalysis has been advanced as an environmentally friendly process *via* simple charge-transfer reactions for the remediation of water pollutants.[85] The electrocatalytic performance is primarily governed by the electrocatalyst, which can accelerate the involved half-cell reactions, generating powerful oxidants (such as $^{\bullet}OH$ on the anode surface and hydrogen peroxide (H_2O_2) on the cathode surface) to degrade or completely mineralize the pollutants, as depicted in Fig. 2c.[86–88] Recently, advanced bio-based IHPCs have shown remarkable electrocatalytic performance for water and wastewater treatment (Table 1). For example, Zhou *et al.* used tea

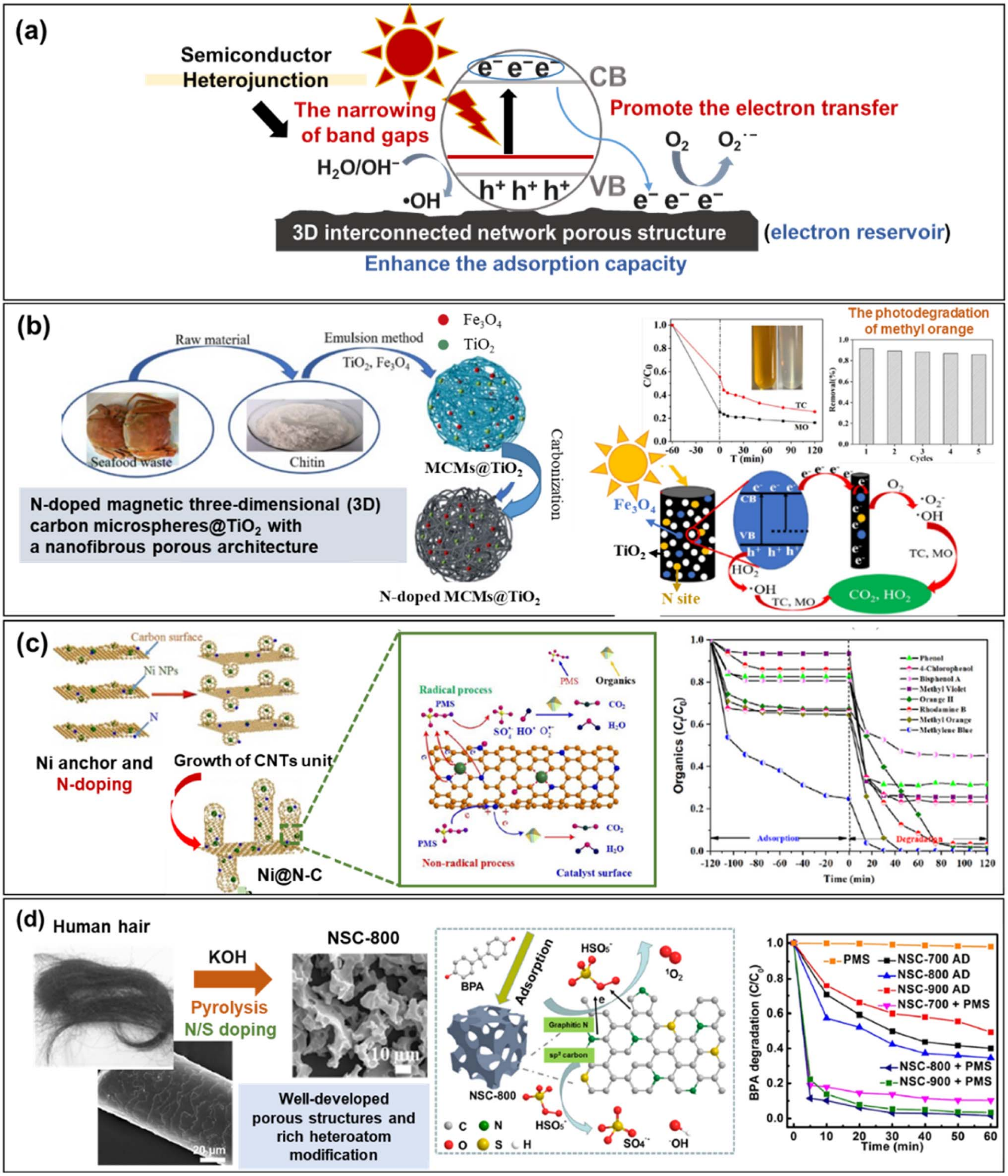

Fig. 3 (a) Schematic diagram of a IHPC catalyst for photocatalysis (information regarding the mechanisms was adopted from ref. 72–74); (b) C/N heteroatom-doped TiO_2/biomass-derived carbon with remarkable stability for organic pollutant degradation under both UV and visible light irradiation (reproduced with permission from ref. 75); (c) nickel embedded in N-doped CNTs supported on biomass-derived porous carbon and (d) human hair-derived N, S-doped porous carbon for sulfate radical-based advanced oxidation processes. Reproduced with permission from ref. 81 and 82, respectively.

leaves to prepare IHPC as a cathode for electrocatalytic degradation of organic pollutants. The hierarchical porous and interconnected microporous structure of tea leaf porous carbon formed a large SSA (1620 m^2 g^{-1}) and increased accessible active sites, thereby promoting electrocatalytic performance. More than 95% of phenol was electrocatalytically degraded by tea leaf-based IHPC.[89] The results indicated that the unique surface properties of bio-based carbon make it a potential candidate in the fields of electrocatalytic degradation.

The introduction of metal oxides, carbides and sulfides on bio-based carbons can further enhance the catalytic activity. Gong *et al.* synthesized a dual-functional material by loading MoS_2 nanospheres and doping O and N on cornstalk-based IHPC (MoS_2/O, N-doped IHPC) as a promising electrode for both cathodic electrocatalytic degradation and supercapacitors. Enhanced catalytic degradation behaviors were proposed, and the degradation performance of phenol (100 mg L^{-1}) reached 97%. The cornstalk-based IHPC served as an efficient electron transfer carrier, and H_2O_2 was generated on its surface *via* the reduction of O_2. O, N and MoS_2 can further accelerate the formation of $^{\bullet}OH$, $^{\bullet}HO_2$ and $O_2{}^{\bullet-}$ (from H_2O_2) to degrade organic pollutants.[90]

Electro-Fenton. The electro-Fenton (EF) process, a typical EAOP, has also been widely researched for organic pollutant degradation. In principle, $^{\bullet}OH$ was generated *via* the catalytic reaction of ferrous iron (Fe^{2+}) with H_2O_2, as shown in Fig. 2d. The electron-Fenton performance is highly dependent on the H_2O_2 production rate and the Fe^{2+} regeneration of the catalysts.[91] Among various catalysts, bio-based IHPC catalysts with surface modification show remarkable H_2O_2 selectivity[92] (Table 1). For example, the H_2O_2 selectivity of an F-doped *Scindapsus aureus*-based IHPC cathode (83%) was much higher than that of a nonmodified IHPC (60%). Additionally, the superior Fe^{2+} regeneration of F-doped IHPC was also evidenced by the reduction peak of Fe^{3+} on F-doped IHPC compared to that on IHPC. The better selectivity of H_2O_2 production and the accelerated recovery of Fe^{2+} of the F-doped IHPC catalyst could facilitate the electro-Fenton degradation of pollutants.[93] N and O self-doped black soybean-based IHPC also showed a high H_2O_2 production rate in the electro-Fenton system, and the degradation efficiency of chloramphenicol reached 100% in 80 min.[73] This superb efficiency indicated that heteroatom-doped bio-based IHPCs show the greatest potential for the electro-Fenton treatment of water pollutants.

4. Bio-based IHPC as a promising adsorbent for water and wastewater treatment

4.1. IHPC for improving water and wastewater treatment efficiency

Removal of toxic trace elements. Heavy metal removal from water/wastewater is of particular interest because most heavy metals are extremely toxic and nonbiodegradable and have the potential to accumulate in human body parts.[94,95] Bio-based IHPC has been systematically explored as a high-potential material for the removal of heavy metals and other toxic trace elements, given its properties of controllable hierarchical porosity and the presence of various surface functional groups.[1,2]

Table 2 introduces the application of IHPC for removal of toxic trace elements. As seen, IHPC can be effectively used to remove various trace elements, such as As, Cr, Pb, Co, Cu, and Cd. Fig. 4a demonstrates the outstanding capabilities of these IHPC adsorbents compared to other commercial materials from previous studies for the removal of As^{3+} (*e.g.*, H_3AsO_3) and As^{5+} (*e.g.*, $H_2AsO_4{}^-$ and $HAsO_4{}^{2-}$),[96–98] Cr^{6+} (*e.g.*, $HCrO_4{}^-$),[99–101] Pb^{2+},[102–104] Cu^{2+},[103,105] Co^{2+},[106,107] Zn^{2+}, and Cd^{2+}.[102] The removal capacities of these ions were comparable or significantly higher than those of other materials from previous studies. For instance, at pH = 2, N-doped IHPC derived from silkworm cocoons showed a high $HCrO_4{}^-$ removal capacity of 366 mg g^{-1},[108] which was much better than that of a $CoFe_2O_4$/commercial activated carbon composite (83.33 mg g^{-1}).[101] The outstanding capabilities of IHPCs in the removal of trace elements are due to the large SSA and high PV, providing abundant surface sites for interacting with pollutants.

Moreover, bio-based IHPCs possess rapid removal rates for trace elements (Table 2). This is because of the 3D pore architecture, which can facilitate pollutant transport from macropores to meso- and micro-pores. For example, Sun *et al.* synthesized an N-doped IHPC adsorbent from a silkworm cocoon by carbonization and activation steps to remove $HCrO_4{}^-$ from wastewater (Fig. S3a†).[108] The IHPC achieved a high SSA (3134 m^2 g^{-1}) and possessed a unique 3D pore architecture, leading to a high adsorption capacity (366 mg g^{-1}) and a fast adsorption rate of Cr(VI) ions (reached equilibrium within 60 min, and 87% of $HCrO_4{}^-$ ions were removed within only 5 min). Yin *et al.* developed O-, N-, and P-doped IHPCs derived from soybean cake and achieved a rapid equilibrium time after 30 min for Pb^{2+} adsorption.[22] Rice husk-based O-rich IHPC obtained equilibrium Cu^{2+} adsorption within 60 min (Cuong *et al.*, 2019).[1] The removal of As by IHPC also exhibited fast speeds, reaching equilibria within 120–180 min.[61,109]

Organic pollutant removal. Recently, bio-based IHPCs have been extensively used for the adsorption of organic compounds such as pesticides, pigments, and pharmaceuticals due to their well-defined 3D pore architecture, high SSA, large PV, and excellent surface chemistry.[110] Studies have shown excellent abilities of bio-based IHPC to adsorb organic contaminants (Table 3). As presented in Fig. 4b, the adsorption capacities of these bio-based IHPC materials are mostly higher than those of other reported materials for methylene blue,[111,112] rhodamine B,[113,114] sulfamethazine,[115,116] chloramphenicol,[117,118] direct black 38,[119] and toluene.[120,121]

Cheng *et al.* produced N-doped fungal slag-based IHPC that possessed an ultrahigh SSA (3342 m^2 g^{-1}) and abundant micropores and mesopores (Fig. S3b†). The obtained IHPC exhibited a high bisphenol A removal capacity of 1249 mg g^{-1} and a rapid removal efficiency of 90% of the equilibrium uptake after 30 min. The IHPC also presented significantly higher removal performance for 2,4-dichlorophenol and methylene blue than commercial activated carbons.[122] Chen *et al.*

Table 2 Application of bio-based IHPC adsorbents for removal of toxic trace elements

Precursor	Ads. temp. (°C)	Ads. pH	Initial conc. (mg L^{-1})	Adsorbent dosage (g L^{-1})	Contact time (h)	Adsorbate	Capacity (mg g^{-1})	Equilibrium time (min)	Isotherm model	Kinetic model	Ref.
Melamine foam (β FeOOH/IHPC)	25	2–10	1–1000	0.5	24	As^{3+}	103	300	—	—	126
Melamine foam (β FeOOH/IHPC)	25	2–10	1–1000	0.5	24	As^{5+}	173	280	—	—	126
Melamine foam (Fe_3O_4/GO@IHPC)	25	2–10	1–1000	1	24	As^{3+}	111	500	L	PSO	127
Persimmon fruit (Fe_3O_4/IHPC)	25	2–9	0.4–2	1	3	As^{5+}	2	120	—	—	109
Bamboo (FeOOH/IHPC)	—	4–12	5	1	5	As^{3+}	—	180	—	—	61
Oil-tea shells (N,P-doped IHPC)	30	2	100, 200	1	24	Cr^{6+}	355	120	L, F, S	PFO, PSO	56
Soybean cake (O, N, and P-doped IHPC)	25	5	60	0.75	2.5	Pb^{2+}	134	30	—	PFO, PSO	22
Silkworm cocoons (N-doped IHPC)	30, 40, 50	2	100–1000	1	10	Cr^{6+}	366	60	L, F	PFO, PSO	108
Banana peel (O, N-doped IHPC)	25	—	100	0.8	24	Cu^{2+}	63	180	L, F	PFO, PSO	2
Banana peel (O, N-doped IHPC)	25	—	100	0.8	24	Co^{2+}	122	180	L, F	PFO, PSO	2
Rice husk (O-doped IHPC)	25	5	10–200	0.35	3	Cu^{2+}	265	60	L, F	PFO, PSO	1
Silkworm cocoon (O, N-doped IHPC)	30	6	100	0.8	—	Pb^{2+}	91	—	L, F	—	58
Silkworm cocoon (O, N-doped IHPC)	30	6	100	0.8	—	Cu^{2+}	87	—	L, F	—	58
Silkworm cocoon (O, N-doped IHPC)	30	6	100	0.8	—	Zn^{2+}	56	—	L, F	—	58
Silkworm cocoon (O, N-doped IHPC)	30	6	100	0.8	—	Cd^{2+}	77	—	L, F	—	58
Silkworm cocoon (O, N-doped IHPC)	30	5	100	0.8	—	Cr^{3+}	51	—	L, F	—	58

employed four kinds of biomass (spruce-pine-fir, maple, bamboo, and cotton) to prepare bio-based IHPC materials and investigated their methylene blue adsorption capacity.[123] Spruce-pine-fir bio-based IHPC achieved a SSA of 729 m^2 g^{-1} and high adsorption capacity of 269 mg g^{-1}, partly due to its highest mesoporous surface area compared to the others. Additionally, the IHPC made from banana peels possessed a high SSA (1397 m^2 g^{-1}), a typical porous structure (0.75 cm^3 g^{-1}) and excellent adsorption capacities for methylene blue and rhodamine B at 744 and 520 mg g^{-1}, respectively.[2] IHPC could be applied for the adsorption of antibiotics.[23,57,124] The IHPC derived from yeast showed promising results with an excellent adsorption removal capacity of sulfamethazine (1244 mg g^{-1}).[124] A high adsorption capacity of sulfamethazine was reported by IHPCs derived from shrimp shells (699 mg L^{-1})[57] and bovine bone (1194 mg L^{-1}).[23]

IHPC is also an excellent material for the removal of volatile organic compounds (VOCs). Tang *et al.* developed a cellulose-derived non-N-doped IHPC and N-doped IHPC for investigating the effect of the 3D pore architecture and N functional groups on toluene and benzene adsorption.[125] The N-doped IHPC presented adsorption capacities for toluene (272 mg g^{-1}) and benzene (151 mg g^{-1}), which were significantly higher than those of non-N-doped IHPC and commercial activated carbon. These researchers confirmed that the 3D pore architecture provided a rapid pathway that was beneficial for adsorbate transport from the surface into inner pores, improving the adsorption rate. Additionally, the N functional groups of N-doped IHPC contributed to the increase in adsorption capacity for toluene.

4.2. Mechanisms for enhanced removal of trace elements

Fig. 5a illustrates the working mechanisms of trace element removal by bio-based IHPC. The mechanisms governing trace element adsorption include physisorption and chemisorption (*i.e.*, electrostatic attraction, ion exchange, surface complexation, and/or precipitation). Surface functional groups on bio-based IHPC surfaces, such as carboxyl (COOH) and hydroxyl (OH) can participate in these mechanisms to remove the trace elements. It should be mentioned that the unique 3D interconnected pore architecture of IHPC consisting of macropores, mesopores, and micropores is important for improving the trace element adsorption capacity and rate. Manufactured IHPC materials usually have micropores in the range from 0.5 to 2 nm, while most trace elements are smaller than 0.5 nm; *e.g.*, the diameters of Cr^{6+}, Cu^{2+}, and Zn^{2+} are 0.116, 0.174, and 0.176 nm, respectively. Therefore, these ions can deeply approach narrow micropores and can be retained on active sites.

Coating the IHPC surface by heteroatom doping or metal (hydr)oxides/hydroxides is a scheme for enhancing the trace element removal efficiency.[126,127] Ge *et al.* synthesized β-FeOOH nanorod/melamine foam-based IHPC for highly effective arsenic removal. The bio-based IHPC achieved remarkably high adsorption capacities of 103.4 mg g^{-1} and 172.9 mg g^{-1} for As^{3+} (*e.g.*, H_3AsO_3) and As^{5+} (*e.g.*, $H_2AsO_4^{-}$ and $HAsO_4^{2-}$), respectively. These high adsorption capacities were attributed to

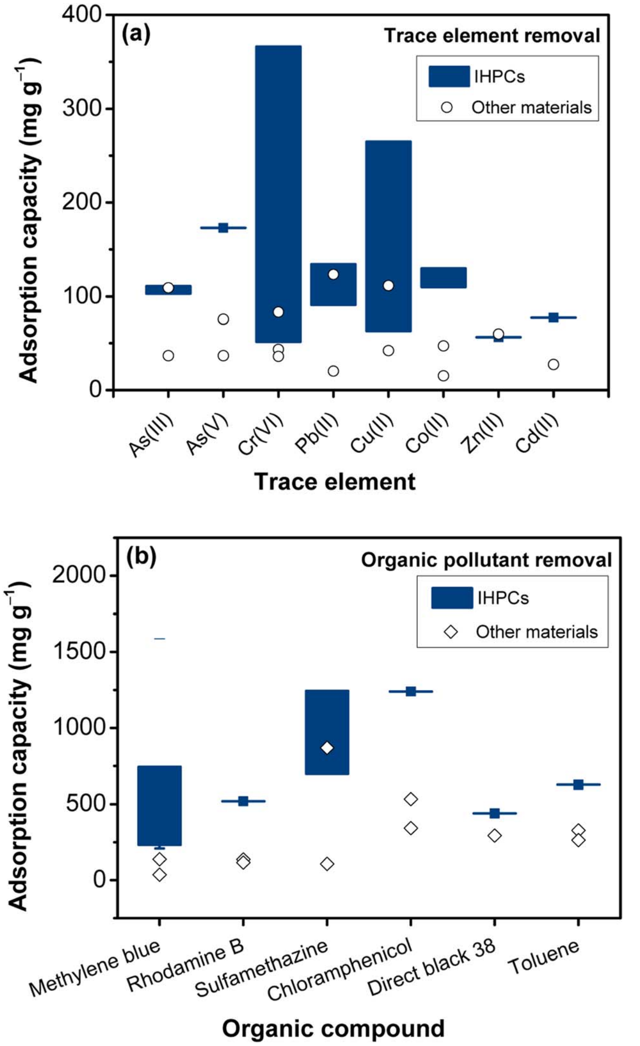

Fig. 4 Comparison of the adsorption capacities of IHCPs (see Tables 2 and 3) to other materials for the removal of (a) trace elements and (b) organic compounds. Symbols (○) represent the trace element adsorption capacities of As^{3+},[96–98] As^{5+},[96,97] Cr^{6+},[99–101] Pb^{2+},[102–104] Cu^{2+},[103,105] Co(II),[106,107] Zn^{2+}, and Cd^{2+}.[102] Symbols (◇) represent the organic adsorption capacities of methylene blue,[111,112] rhodamine B,[113,114] sulfamethazine,[115,116] chloramphenicol,[117,118] direct black 38,[119] and toluene.[120,121]

efficient mass transfer associated with 3D interconnected hierarchical pore networks, as well as the presence of large numbers of active sites and hydroxyl functional groups from β-FeOOH modification. Importantly, As species can be adsorbed on the bio-based IHPC surface *via* surface complexation and ion exchange with hydroxyl groups.[126]

N,P-codoped IHPC derived from the oil-tea shell exhibited a high $HCrO_4^-$ adsorption capacity of 355 mg g^{-1}.[56] The excellent adsorption performance of IHPC was attributed to the accommodation of $HCrO_4^-$ ions inside the hierarchical porous structure of the IHPC. On the other hand, the chemisorption of $HCrO_4^-$ is governed by electrostatic attraction, reduction, and precipitation mechanisms.[128,129] The outstanding performance of N-doped silkworm cocoon-based IHPC was because the O-containing functional groups and the high content of pyrrolic N on the IHPC further contributed to the promotion of chemisorption of $Cr_2O_7^{2-}$ ions.[108] Moreover, the electrostatic attraction between the negative charge of Cr(VI) (such as $HCrO_4^-$, $Cr_2O_7^{2-}$, and CrO_4^{2-}) and the positively charged surface of the IHPC played an important role in favoring the adsorption of Cr^{6+}. Furthermore, burcucumber-based IHPC has the potential to be a promising redox-active material for converting $Cr_2O_7^{2-}$ into Cr^{3+} with various O-containing surface functional groups, *e.g.*, phenolic, carbonyl, and carboxyl.[128] A soybean cake-based IHPC was fabricated with a variety of functional groups formed from heteroatom elements (O, N, and P) and silanol groups, and it achieved a high Pb^{2+} removal capacity of 134 mg g^{-1}.[22] These functional groups may provide an abundance of active sites as well as improved wetting properties to achieve a larger ion-accessible surface area. In addition, the silicon and silanol O groups reacted with Pb^{2+} *via* surface complexation.

4.3. Mechanisms for the enhanced removal of organic compounds

Fig. 5b depicts the working mechanisms of organic compound removal by bio-based IHPC. Note that the molecular sizes of most organic compounds are significantly larger than those of trace elements. The adsorption of organic compounds by the pore-filling mechanism is strongly correlated with the pore size. The adsorption capacity of an adsorbent for an organic compound (C_{exp}) can be estimated by using the following equation:[123]

$$C_{\mathrm{exp}} = C_{\mathrm{inE}} \times \text{InE-SSA} + C_{\mathrm{E}} \times \text{E-SSA}$$

where InE-SSA and E-SSA are defined as the ineffective and effective SSA of pores, which are smaller and larger than the size of the organic compound, respectively. C_{inE} and C_{E} are the adsorption capacities contributed by the unit InE-SSA (mg g^{-1}) and E-SSA (mg g^{-1}), respectively. Similarly, it was reported that the low utility of pores was considered in the adsorption of larger diameter pollutants. The adsorption capacity of phenol or tannic acid on activated carbon increases with increasing mesoporosity.[130] Most micropores in activated carbon are inaccessible for organic compound removal.[131]

The chemical adsorption of organic pollutants by bio-based IHPC can be governed by electrostatic interactions, π–π stacking, and hydrogen bonding, as shown in Fig. 5b.[2,57,132,133] Bio-based IHPCs usually have negatively charged surfaces because of the existence of O-containing functional groups. Cationic organic compounds can be adsorbed easily by electrostatic forces on negatively charged surfaces of IHPC.[123] The N or/and S contents inside IHPC may function as the hydrogen-bonding acceptor, allowing the formation of hydrogen bonds between the hydroxyl group on the IHPC surface and organic compounds.[2] The addition of OH groups can greatly enhance the affinity of carbon materials and organic molecules due to two hydrogen-bonding interactions. Inserting metals/metal oxides/metal hydroxides can improve organic separation. For example, MgO modification enhanced the binding energy between the IHPC surface and the acetone molecule more than five times that

Table 3 Application of bio-based IHPC adsorbents for organic compound removal[a]

Precursor	Ads. temp. (°C)	Ads. pH	Initial conc. (mg L^{-1})	Adsorbent dosage (mg L^{-1})	Contact time (h)	Adsorbate	Capacity (mg g^{-1})	Equilibrium time (min)	Isotherm model	Kinetic model	Ref.
Spruce-pine-fir (O-doped IHPC)	25	1–12	—	1	12	Methylene blue	269	—	L	—	123
Maple fir (O-doped IHPC)	25	1–12	—	1	12	Methylene blue	233	—	—	—	123
Bamboo fir (O-doped IHPC)	25	1–12	—	1	12	Methylene blue	209	—	—	—	123
Cotton fir (O-doped IHPC)	25	1–12	—	1	12	Methylene blue	242	—	—	—	123
Banana peel (O, N-doped IHPC)	25	—	800	0.8	24	Methylene blue	744	240	L, F	PFO, PSO	2
Banana peel (O, N-doped IHPC)	25	—	800	0.8	24	Rhodamine B	520	240	L, F	PFO, PSO	2
Shrimp shell fir (N-doped IHPC)	25–45	3–9	280	0.3	3	Sulfamethazine	699	180	L, F	PFO, PSO, IPD	57
Shrimp shell (N-doped IHPC)	25–45	3–9	280	0.3	3	Chloramphenicol	742	180	L, F	PFO, PSO, IPD	57
Yeast	25	6	300	0.2	12	Sulfamethazine	1244	60	L, F	PFO, PSO, IPD	124
Bovine bone (O, N-doped IHPC)	25–45	—	200	0.2	12	Sulfamethazine	1194	180	L, F	PFO, PSO	23
Bovine bone (O, N-doped IHPC)	25–45	—	200	0.2	12	Chloramphenicol	1240	180	L, F	PFO, PSO	23
N-doped fungus slag-based IHPC	15	5	500	0.1	7	Bisphenol A	1249	30	L, F	PFO, PSO	122
N-doped fungus slag-based IHPC	15	5	500	0.1	7	2,4-Dichlorophenol	1155	30	L, F	PFO, PSO	122
N-doped fungus slag-based IHPC	15	5	500	0.1	7	Methylene blue	869	30	L, F	PFO, PSO	122

[a] L and F are Langmuir and Freundlich isotherm models, respectively; PFO, PSO and IPD are pseudo-first, pseudo-second and intraparticle-diffusion kinetic models, respectively.

of the one without modification. This is ascribed to the Lewis acid–base interaction of MgO with acetone molecules.[63]

5. Bio-based IHPC as a promising adsorbent for carbon capture

5.1. IHPC for improving carbon capture performance

Climate change is one of the most pressing challenges in the world. Carbon dioxide (CO_2), accounting for 81% of greenhouse gases, is a major contributor to global warming, causing enormous impacts on the global ecosystem.[134,135] Additionally, methane (CH_4) is not only a major greenhouse gas (accounting for 10%) but also a potential energy source.[60] CH_4 is a byproduct of mining and transporting coal, natural gas, and oil. CH_4 emissions can also be generated by livestock and agricultural activities and the decomposition of organic waste in municipal solid waste landfills. Incomplete combustion of fossil fuels in the operation of vehicles, power plants and other human activities results in the emission of CO_2 and other pollutants (*e.g.*, CO, SO_x, NO_x, N_2O and VOC_s).

Carbon adsorbents are known as some of the most commonly used materials for carbon capture.[135–139] Note that the desired geometry, PV, and SSA of carbon materials are crucial for achieving high carbon capture efficiency.[140,141] Notably, Table 4 presents various applications of bio-based IHPCs for carbon capture, *i.e.*, CO_2 and CH_4. For instance, Tian *et al.* synthesized an algae-based IHPC with an SSA of only 416 m^2 g^{-1} and a mesoporosity of 70%.[33] The IHPC showed a higher CO_2 uptake of 6.48 mmol g^{-1}.

The utilization of water chestnuts to prepare IHPC for CO_2 capture was demonstrated by Wei *et al.*[142] An ultrahigh SSA (3401 m^2 g^{-1}) and rich N content (4.89 at%) significantly contributed to the CO_2 capture capacity, which can achieve 6.0 mmol g^{-1} and 4.7 mmol g^{-1} at 0 °C and 25 °C under 0.1 MPa, respectively. Poplar catkin-based N-doped IHPC microtubes were fabricated by Chang *et al.*[55] (Fig. S4a and b†). Most notably, the presence of numerous micropores and N species was responsible for a significant performance in CO_2 adsorption. The IHPC exhibited a CO_2 capture capacity of 6.22 mg g^{-1} at 0 °C under 0.1 MPa, respectively. Moreover, the IHPC had high selectivity and recyclability for CO_2 capture compared to N_2. The applications of bio-based IHPCs for efficient gas-mixture separation have been of interest to many researchers. Liu *et al.* fabricated controllable heteroatom-doped IHPC for investigating the selectivity of CO_2 in mixture gases (Fig. S4c and d†). The IHPC indicated excellent CH_4/N_2, CO_2/CH_4, and CO_2/N_2 selectivities of 7.6, 10.7, and 107 at 25 °C and 1.0 bar, respectively.[60] A higher selective ratio of CO_2 over other gases resulted in a higher carbon capture capacity, contributing to the reduction of climate change.

The 3D pore architecture of IHPC is most important and has a direct relationship with the CH_4 adsorption capacity. Note that ultramicropores with narrow pore size distributions benefit CH_4 capture.[60] Corncob-derived IHPC has a high SSA (3227 m^2 g^{-1}) and large PV (1.83 cm^3 g^{-1}). In the presence of water, the CH_4 capture was 43.7 wt% CH_4/unit mass of the dry HPC at 2 °C

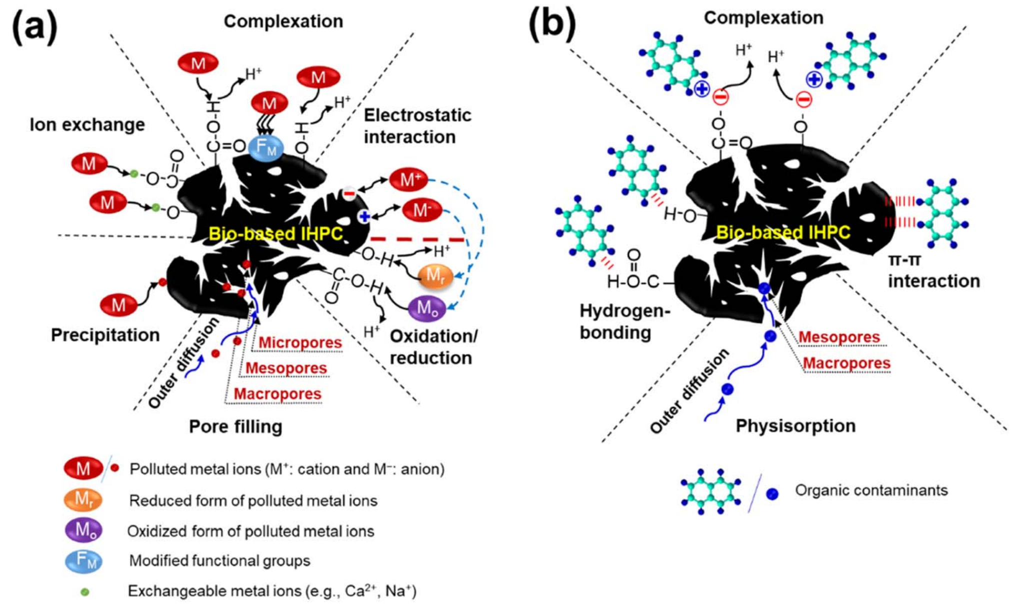

Fig. 5 Working mechanisms for the removal of (a) metal ions[11,19,56,126–129] and (b) organic compounds[2,57,123,132] *via* bio-based IHPCs.

and 78 bar. Corncob-derived HPC is considered a potential CH_4 storage material.[143] Doping N and O atoms on IHPC is also beneficial for CH_4 capture because it can improve the surface polarity of the material. N,O-doped palm sheath-derived IHPC showed a high CH_4 adsorption capacity of 2.27 mmol g^{-1} at 0 °C and 1.0 bar.[60] Under the same conditions, N-doped algae-based IHPC achieved a CH_4 capture capacity of 2.0 mmol g^{-1}.[54]

5.2. Mechanisms for enhancing carbon capture

Given that CO_2 accounts for the majority of greenhouse gases (81%), increasing CO_2 storage is regarded as the most effective solution in efforts to mitigate climate change. As a result, the review attempts to delve deeper into the potential for efficiency improvements as well as the critical mechanisms of CO_2 capture. Fig. 6a compares the CO_2 uptake capacity of bio-based IHPC with other materials. The CO_2 uptake capacities of bio-based IHPCs are significantly higher than those of IHPC derived from commercial precursors[144–149] and CNTs, granular activated carbons and zeolites.[150] This finding may be due to the integration of the 3D pore architecture design and chemical doping on bio-based IHPC, providing facilitated pathways and abundant active sites for the transport and capture of CO_2 molecules.

The CO_2 capture mechanisms by bio-based IHPC comprise physisorption and chemisorption (Fig. 6b). In the physisorption mechanism, micropores play an imperative role by providing active sites, which generate interactions with CO_2 molecules by relatively weak van der Waals forces. Chang *et al.* observed that the CO_2 uptake capacity had a linear relationship with the micropore volume of poplar catkin-based IHPC (Fig. S4b†). This observation indicates that CO_2 adsorption mainly occurred in the micropores, while macropores and mesopores facilitate rapid diffusion of CO_2 molecules into the carbon matrix.[55]

CO_2 chemisorption can be accomplished by the involvement of functional groups on the outer surface of the IHPC.[142] Note that acidic molecules, such as CO_2, favor surface basicity strictly. Therefore, basic O-functional groups, including hydroxyl, pyrone, chromene, and diketone/quinone groups, can

Table 4 Application of bio-based IHPC adsorbents for carbon capture

Precursor	Ads. temp. (°C)	Pressure (bar)	Adsorbate	Capacity (mmol g^{-1})	Ref.
Chestnut (N-doped IHPC)	0/25	1	CO_2	6.0/4.7	142
Algae	25	20	CO_2	6.48	33
Poplar catkin (N-doped IHPC)	0/25	1	CO_2	6.22/4.05	55
Algae (N-doped IHPC)	0/25	1	CO_2	5.7/3.9	54
Algae (N-doped IHPC)	0/25	1	CH_4	2.0/1.3	54
Agro-waste		—	CO_2	6.8/4.5	140
Sunflowers	0/25	—	CO_2	4.52/3.08	141
Palm sheath (N, O-doped IHPC)	0/25	—	CO_2	5.78/4	60
Palm sheath (N, O-doped IHPC)	0	—	CH_4	2.27	60
Pigskin collagen	0/25	1	CO_2	5.3/4.4	139
Date sheets	0/25	—	CO_2	6.4/4.36	24

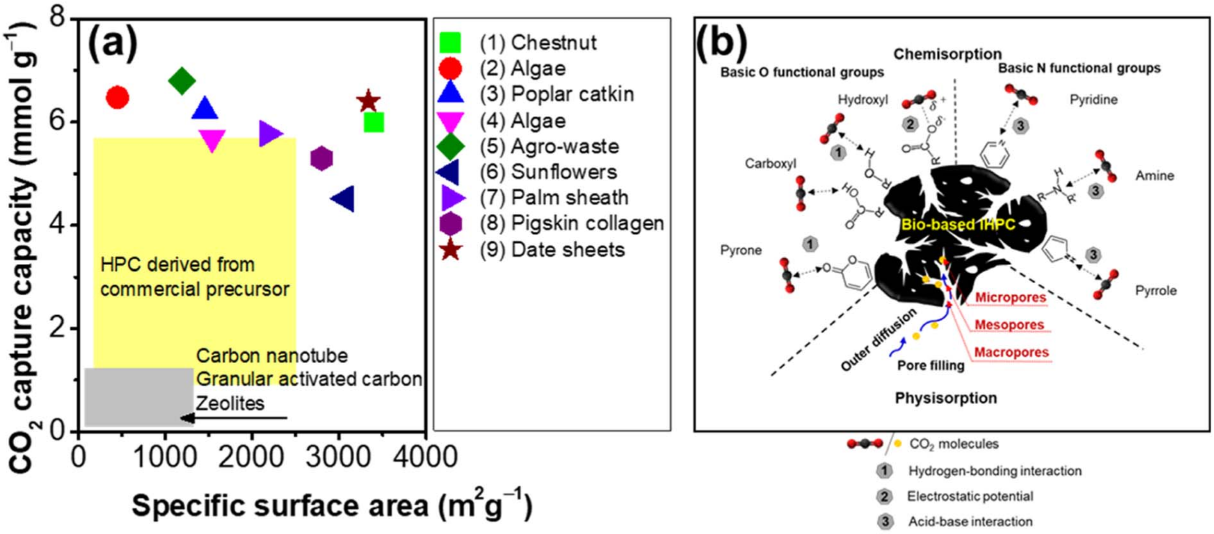

Fig. 6 (a) Comparison of the CO_2 capture capacity of bio-based IHPCs derived from (1) chestnut,[142] (2) algae,[33] (3) poplar catkin,[55] (4) algae,[54] (5) agro-waste,[140] (6) sunfalls,[141] (7) palm sheaths,[60] (8) pigskin collagen,[139] and (9) date sheets[24] to that of other materials, such as HPCs derived from commercial precursors,[144–149] carbon nanotubes, granular activated carbons and zeolites[150] and (b) working mechanisms of CO_2 capture *via* bio-based IHPC. Information regarding mechanisms was summarized from ref. 12, 55, 135, 142 and 151.

enhance the uptake of CO_2.[12] As reported, CO_2 capture is largely dependent on the hydroxyl group, and the capacity increases with increasing content. This behavior occurs because the hydroxyl groups interact with the CO_2 molecule *via* hydrogen-bonding interactions and electrostatic potentials.[151] However, the O-functional groups on IHPC often generate hydrogen bonds with water molecules in humid environments, thereby enhancing hydrophilicity. The enhanced hydrophilicity of IHPC causes competition between moisture and CO_2 adsorption, resulting in a reduction in the CO_2 adsorption capacity.

Basic N-containing functional groups on bio-based IHPCs, *e.g.*, pyridine, amines, anilines, and pyrrole, are important in the adsorption of CO_2 due to the affinity between these functional groups and CO_2 *via* acid–base interactions.[152] Note that the CO_2 adsorption capacity of IHPC is proportional to the micropore surface area at a lower temperature. However, the CO_2 adsorption capacity depends on the N content of IHPC at a higher temperature.[153] The IHPC offers superior thermal stability, tunable pore structure, and high chemical resistance, while the IHPC with interconnected micro/mesopores exhibited promising results for CO_2 capture. Zhang *et al.* reported a simple and cost-effective method for synthesizing IHPC materials with significant micropores for CO_2 capture applications. The results revealed high CO_2 uptake attributed to the developed abundant interconnected micro/mesopores.[154] The optimization of porosity formation with other physicochemical properties of bio-based IHPCs can offer a promising direction for excellent selective CO_2 capture on a commercial scale in the future.

6. Expanding the environmental applications of bio-based IHPC

Bio-based IHPC accelerants, with their unique 3D architecture design and chemical doping, have shown significant potential in enhancing AD processes. The 3D architecture design of IHPC accelerants provides a highly porous structure with a large surface area, allowing for improved mass transfer and microbial colonization. This enhanced contact between the substrate and microorganisms increases the efficiency of organic matter degradation and biogas production. Furthermore, chemical doping of IHPC accelerants with specific elements or compounds can enhance their catalytic activity and promote the decomposition of complex organic compounds found in the feedstock. The synergistic effects of the 3D architecture design and chemical doping contribute to increased biogas yields and improved overall performance of anaerobic digestion systems. These advancements in bio-based IHPC accelerants offer promising opportunities for optimizing anaerobic digestion processes and increasing the utilization of organic waste as a renewable energy source.[25,155–157] For instance, Chen *et al.* introduced Co_3O_4/aloe peel-derived IHPC as an accelerant, leading to a remarkable increase in the cumulative biogas yield (577 mL g^{-1} VS) and an enhanced total chemical oxygen demand degradation rate (70.45%) compared to a control group without accelerants (435.8 mL g^{-1} VS, 50.74%).[4] The improved AD performance, as reported by Li *et al.*, can be attributed to the application of N, P co-doped aloe peel-derived IHPC accelerants. This resulted in favorable methane production (350.21 mL g^{-1} VS), cumulative biogas production (526.77 mL g^{-1} VS), and a significant total chemical oxygen demand degradation rate of 80.19%. The formation of functional groups on the surface of the material played a crucial role in facilitating electron exchange capacity and adsorption capability, thus contributing to enhanced AD performance.[158]

Bio-based IHPC with 3D architecture design and chemical doping also represents a promising avenue for advanced antimicrobial treatment.[159] The porous structure offers a large surface area for increased adsorption of harmful microbes, while the 3D architecture allows for efficient mass transfer and improved mechanical stability. Moreover, chemical doping of the carbon matrix with antimicrobial agents further enhances its efficacy by introducing additional antibacterial properties. For example, Wang *et al.* successfully produced garlic-derived CDs with self-doped nitrogen and sulfur. When tested against various strains, CDs exhibited minimum inhibitory concentrations of 25, 75, and 50 μg mL^{-1} against methicillin-resistant *Staphylococcus aureus*, multidrug-resistant *Salmonella typhimurium*, and generic *Escherichia coli*, respectively. Remarkably, CDs at a concentration of 200 μg mL^{-1} completely eradicated all three bacteria strains within a span of 180 minutes.[160] The antimicrobial properties of CDs derived from an extract of *Syzygium cumini* L., a medicinal seed, were investigated. At a concentration of 500 μg mL^{-1}, the CDs exhibited significant antimicrobial activity against four prevalent pathogens of *S. aureus*, *S. epidermidis*, *E. coli* and *Klebsiella pneumonia*. It is hypothesized that the release of various reactive oxygen species contributes to the mechanism of bacterial eradication.[161] The remarkable antimicrobial properties of the IHPC nanocomposite derived from *Coccinia grandis* peel, which includes silver, were demonstrated against both Gram-negative and Gram-positive bacteria. It effectively targeted *E. coli*, *Pseudomonas aeruginosa*, *Bacillus subtilis*, and *S. aureus*. The incorporation of silver nanoparticles in IHPC seemed to enhance its antibacterial effectiveness.[162]

By combining bio-based porous carbon with 3D architecture design and chemical doping, it is possible to develop highly efficient and selective materials for oil–water separation. These materials can be used in diverse settings, such as wastewater treatment, oil spill cleanup, or industrial separation processes, to separate and recover oil from water effectively. These materials can be processed and engineered to have a hierarchical 3D architecture, which enhances their performance in oil–water separation. The 3D architecture provides interconnected pathways for fluids to flow through, maximizing contact between the porous carbon and the oil–water mixture.[163,164] Chemical doping involves introducing dopant materials into the carbon structure to modify its properties. Doping can enhance the hydrophobicity or oleophilicity of the porous carbon, making it more effective in selectively adsorbing oil from oil–water mixtures. According to Varshney *et al.*, a material derived from guava leaves was synthesized for the purpose of separating crude oil from oil–water mixtures through absorption. At room temperature, the material demonstrated an impressive separation efficiency of approximately 98%, along with an oil absorption capacity of approximately 1291 wt%.[26] A new composite material consisting of 3D polydimethylsiloxane modified MoS_2@biomass-derived carbon was developed by Xu *et al.* This innovative composite demonstrated outstanding hydrophobic and oleophilic characteristics, along with a remarkable adsorption capacity for oil, reaching up to 98.5%. Furthermore, even after undergoing 10 cycles, the material retained a high oil-absorption capacity, indicating its excellent recoverability and reusability.[165]

7. Future prospects of bio-based IHPC

Bio-based IHPC has demonstrated significant potential as an adsorbent and catalyst for water and wastewater treatment, as well as carbon capture. However, there are several challenges associated with its application. A primary obstacle lies in achieving scalability and reproducibility in the synthesis of bio-based IHPC. Large-scale production of IHPC with consistent properties and performance is hindered by variations in biomass feedstock, pyrolysis conditions, and activation processes. Moreover, the choice of biomass feedstock for IHPC production introduces significant variability in terms of composition, quality, and properties. Different types of biomass, such as agricultural waste, lignocellulosic materials, or algae, can result in IHPC with varying pore structures and surface chemistries. This variability poses a challenge in establishing consistent performance across different feedstocks, as it can directly impact the catalytic activity and adsorption performance of IHPC. While bio-based IHPC has exhibited promising performance in laboratory-scale studies, its effectiveness under real-world conditions requires further exploration. Factors such as the presence of impurities, competing ions, and complex matrices in water and wastewater can influence the adsorption capacity and catalytic activity of IHPC. Understanding the performance of IHPC in practical scenarios, including long-term stability and regeneration potential, is crucial for its successful application in large-scale water treatment and carbon capture processes.

To overcome these challenges, novel approaches and research directions are needed. Firstly, selecting exceptional biomass precursors can enhance the quality and performance of IHPC. Secondly, exploring the use of natural materials to produce low-cost IHPC from biomass can contribute to cost reduction. Thirdly, controlling IHPC qualities, such as pore structure, chemical doping, and stability, can lead to highly efficient performance in environmental remediation applications. Lastly, considering factors relevant to applying bio-based IHPC in practical conditions will help bridge the gap between laboratory-scale success and real-world implementation. By pursuing these research directions, it is expected that the fabrication cost of IHPCs can be reduced, and their efficiency for real applications can be improved.

First, selecting exceptional biomass precursors is a crucial step. The discovery of new biomass materials with outstanding properties (*e.g.*, low cost, large storage and rich surface functional groups) is still needed to fabricate technically and economically efficient IHPCs. Multiple-criteria decision analysis (MCDA) should be used to select outstanding biomass for preparing IHPC. Criteria such as the C content, functional groups (*e.g.*, O and N), cost, storage, structure, and other special properties (*e.g.*, available template) can be used in evaluating options to select the best biomass for each target application. For example, biomass with high C components, such as chestnut, oak wood, walnut shell and coconut shell, provides IHPC with a highly porous structure (*e.g.*, SSA, PV and meso-/micropore ratio) and higher yield. More specifically, biomass with a high available N content (*e.g.*, soybean, silkworm cocoon, and algae) often provides rich N functional groups for doping IHPC. Other functional groups (*e.g.*, sulfur) containing in biomass should be discovered and evaluated for the effect on the efficiency of IHPC applications.

Second, exploring the use of natural materials to produce low-cost IHPC from biomass is an alternative to commercial chemicals. The search for alternative natural materials to use as catalysts, templates, activators, and doping precursors and the use of a green process are both encouraged in the fabrication of IHPCs. Controlling the porosity development by using the template method is necessary for producing highly porous IHPC. The self-template method with a natural template (*e.g.*, SiO_2 in rice husk) should be considered to fabricate low-cost IHPCs. Chemical agents such as NaOH, KOH, and H_3PO_4 are most commonly used for the activation process. Although these activation agents are effective for the development of porosity, they are usually expensive and nonenvironmentally friendly choices. Using self-activated biomass (*e.g.*, $CaCO_3$ in oyster shells) or natural materials (*e.g.*, orange peel) and green chemicals (*e.g.*, $CaCl_2$) as feedstock can provide a green activation process. Notably, using biomass or a natural precursor containing rich functional groups (*e.g.*, O, N…) as the doping precursor to prepare IHPC is suggested for further studies. Highly porous O/N-doped IHPC can be fabricated by combining multiple biomass materials with different properties, which either contain a high C content to develop porosity or rich O/N functional groups for doping processes. An appropriate ratio of chemical doping (*e.g.*, O and N functional groups, metal oxides and hydroxides) also needs to be evaluated to optimize the doping process.

Third, to achieve the best performance for environmental remediation, the uniform quality of the bio-based IHPC catalyst and adsorbent, such as the size, morphology, and distribution of additive compounds in the modification step, must be well controlled. The longevity of bio-based IHPCs is critical for developing new applicable materials and should be investigated. A new research strategy in catalysis for environmental remediation, such as the integration of electrocatalysts and electrosorption, is also an attractive direction. Note that the removal efficiency of pollutants by adsorption depends on the transportation of ions or molecules in the macro- and mesoporous channels of bio-based IHPCs. It has a strong relationship with the pore size distribution of bio-based IHPCs and pollutant size, particularly organic compounds. It is critical to understand the relationships among the pollutant removal efficiency, the pore size distribution of bio-based IHPCs, and pollutant size. Furthermore, specific modifications (for example, coating MnO_2 for As(III) oxidation) should be extensively carried out to improve the adsorption capacity of bio-based IHPCs. Studies involving the assessment of the individual contributions of the hierarchical pore structure and surface functional groups of IHPC should be performed.

Fourth, emerging applications of bio-based IHPCs should be performed with a field-pilot study to determine the economic, technical, and environmental feasibility. The adoption of companies and production facilities is the main barrier to scaling up the use of biochar for IHPC production. National policies (*i.e.*, tax deductions) can be a powerful tool for encouraging the use of biomass as a precursor. Furthermore, future research should focus on the use of bio-based IHPC catalysts and adsorbents for the treatment of multicomponent mixtures, real industrial effluents, or natural water and regeneration, as well as fixed-bed column studies. It is necessary to assess the selectivity/competitiveness of ions in real water/wastewater. It should also consider the possible complexation formation of trace elements and the effect on their treatment efficiencies in real aqueous environments.

8. Conclusion

This review offers a deep understanding of engineered catalysts and adsorbents derived from biomass, which are designed with unique 3D pore architecture and chemical doping surfaces (denoted as bio-based IHPCs) for environmental applications. Bio-based IHPC is a renewable, environmentally friendly and cost-effective material. The 3D interconnected pore architecture including micro, meso-, and macro-pores of IHPC is advantageous for matter transport. The pore architecture of bio-based IHPCs can be designed using non-templating, hard-templating, and self-templating strategies. Chemical doping on the surface of bio-based IHPCs can be performed by loading metals/metal oxides/hydroxides or heteroatoms (O, N, P, *etc.*). The chemical doping steps can provide more active sites for surface or interface-related processes between IHPC and pollutants. As a result, bio-based IHPCs are promising engineered catalysts and adsorbents for removing heavy metals and organic compounds in water and wastewater, and carbon capture (*e.g.*, CO_2 and CH_4). Additionally, the discussion encompassed the exploration of bio-based IHPC's extended environmental applications in optimizing anaerobic digestion processes, improving antimicrobial treatment and enhancing oil–water separation. This review offers insights into the mechanisms of bio-based IHPCs for the catalysis and adsorption of pollutants. From a future perspective, biomass utilization for preparing IHPC with desirable physicochemical properties by environmentally friendly processes were encouraged to prepare a high-performance catalyst/adsorbent. Further research on the regeneration, scaling up, and selectivity/competitiveness of ions in real water/wastewater should be conducted before IHPC can be used in practice.

Author contributions

Dinh Viet Cuong: conceptualization, methodology, investigation, writing – original draft, and funding acquisition; Jhen-Cih Wu: conceptualization, writing – original draft, and visualization; Eakalak Khan: writing – review & editing; Gijs Du Laing: writing – review & editing; Yong Sik Ok: conceptualization, writing – review & editing, supervision, and project administration; Chia-Hung Hou: conceptualization, writing – review & editing, supervision, and funding acquisition.

Conflicts of interest

There are no conflicts to declare.

Acknowledgements

This research was funded by the Ministry of Science and Technology, Taiwan (109-2223-E-002-002-MY3), the National Taiwan University (NTU) Research Center for Future Earth from the Featured Areas Research Center Program within the framework of the Higher Education Sprout Project by the Ministry of Education (MOE) in Taiwan, the Ministry of Education & Training, Vietnam (B2022-XDA-01) and the Hanoi University of Civil Engineering, Vietnam for Research Group No. 10-Nano-Assisted CDI (07-NNC-DHXDHN). This work was carried out with the support of the Cooperative Research Program for Agriculture Science and Technology Development (Project No. PJ01475801) from Rural Development Administration, the Republic of Korea. This work was supported by the National Research Foundation of Korea (NRF) grant funded by the Korea government (MSIT) (No. 2021R1A2C2011734). This research was supported by Basic Science Research Program through the National Research Foundation of Korea(NRF) funded by the Ministry of Education (NRF-2021R1A6A1A10045235). This work was supported by the National Research Foundation of Korea (NRF) grant funded by the Korea government (MSIT) (NRF-2022M3J4A1091450). This work was supported by OJEong Resilience Institute, Korea University.

References

1 D. V. Cuong, N. L. Liu, V. A. Nguyen and C. H. Hou, Meso/micropore-controlled hierarchical porous carbon derived from activated biochar as a high-performance adsorbent for copper removal, *Sci. Total Environ.*, 2019, **692**, 844–853.

2 D. Y. Yu, L. L. Wang and M. H. Wu, Simultaneous removal of dye and heavy metal by banana peels derived hierarchically porous carbons, *J. Taiwan Inst. Chem. Eng.*, 2018, **93**, 543–553.

3 H. Cheng, Y. Sun, X. Wang, S. Zou, G. Ye, H. Huang and D. Ye, Hierarchical porous carbon fabricated from cellulose-degrading fungus modified rice husks: Ultrahigh surface area and impressive improvement in toluene adsorption, *J. Hazard. Mater.*, 2020, 122298.

4 J. Chen, S. Yun, J. Shi, Z. Wang, Y. Abbas, K. Wang, F. Han, B. Jia, H. Xu, T. Xing and B. Li, Role of biomass-derived carbon-based composite accelerants in enhanced anaerobic digestion: Focusing on biogas yield, fertilizer utilization, and density functional theory calculations, *Bioresour. Technol.*, 2020, **307**, 123204.

5 M. Tariq, A. Singh, N. Varshney, S. K. Samanta and M. P. Sk, Biomass-derived carbon dots as an emergent antibacterial agent, *Mater. Today Commun.*, 2022, **33**, 104347.

6 S. Dutta, A. Bhaumik and K. C. W. Wu, Hierarchically porous carbon derived from polymers and biomass: effect of interconnected pores on energy applications, *Energy Environ. Sci.*, 2014, **7**, 3574–3592.

7 C. J. Yuan, H. B. Lin, H. Y. Lu, E. D. Xing, Y. S. Zhang and B. Y. Xie, Synthesis of hierarchically porous MnO_2/rice husks derived carbon composite as high-performance electrode material for supercapacitors, *Appl. Energy*, 2016, **178**, 260–268.

8 O. Karatum, S. A. Steiner III, J. S. Griffin, W. Shi and D. L. Plata, Flexible, mechanically durable aerogel composites for oil capture and recovery, *ACS Appl. Mater. Interfaces*, 2016, **8**, 215–224.

9 K. Y. A. Lin, H. A. Chang and B. J. Chen, Multi-functional MOF-derived magnetic carbon sponge, *J. Mater. Chem. A*, 2016, **4**, 13611–13625.

10 D. V. Cuong, P.-C. Wu, S. Y. H. Liou and C.-H. Hou, An integrated active biochar filter and capacitive deionization system for high-performance removal of arsenic from groundwater, *J. Hazard. Mater.*, 2022, **423**, 127084.

11 A. U. Rajapaksha, S. S. Chen, D. C. W. Tsang, M. Zhang, M. Vithanage, S. Mandal, B. Gao, N. S. Bolan and Y. S. Ok, Engineered/designer biochar for contaminant removal/immobilization from soil and water: Potential and implication of biochar modification, *Chemosphere*, 2016, **148**, 276–291.

12 D. Saha and M. J. Kienbaum, Role of oxygen, nitrogen and sulfur functionalities on the surface of nanoporous carbons in CO_2 adsorption: A critical review, *Microporous Mesoporous Mater.*, 2019, **287**, 29–55.

13 H. Wang, M. Qu, S. Wang, X. Liu and L. Li, Fabrication of high-performance biomass derived carbon/metal oxide photocatalysts with trilevel hierarchical pores from organic–inorganic network, *Adv. Sustainable Syst.*, 2019, **3**, 1800169.

14 Z. Wan, Y. Sun, D. C. W. Tsang, E. Khan, A. C. K. Yip, Y. H. Ng, J. Rinklebe and Y. S. Ok, Customised fabrication of nitrogen-doped biochar for environmental and energy applications, *Chem. Eng. J.*, 2020, **401**, 126136.

15 V. C. Dinh, C.-H. Hou and T. N. Dao, O, N-doped porous biochar by air oxidation for enhancing heavy metal removal: The role of O, N functional groups, *Chemosphere*, 2022, **293**, 133622.

16 T. Zhu, D. Liu, L. Shi, S. Lu, Y. Gao, D. Zhang, H. Mao, Z. Sun, C.-Y. Lao and M. Li, Nitrogen-doped hierarchical porous carbon-promoted adsorption of anthraquinone for long-life organic batteries, *ACS Appl. Mater. Interfaces*, 2020, **12**, 34910–34918.

17 A. M. Abioye and F. N. Ani, Recent development in the production of activated carbon electrodes from agricultural waste biomass for supercapacitors: A review, *Renewable Sustainable Energy Rev.*, 2015, **52**, 1282–1293.

18 D. V. Cuong, P.-C. Wu, L.-I. Chen and C.-H. Hou, Active MnO_2/biochar composite for efficient As(III) removal: Insight into the mechanisms of redox transformation and adsorption, *Water Res.*, 2021, **188**, 116495.

19 M. I. Inyang, B. Gao, Y. Yao, Y. Xue, A. Zimmerman, A. Mosa, P. Pullammanappallil, Y. S. Ok and X. Cao, A review of biochar as a low-cost adsorbent for aqueous heavy metal removal, *Crit. Rev. Environ. Sci. Technol.*, 2016, **46**, 406–433.

20 M. H. To, K. Uisan, Y. S. Ok, D. Pleissner and C. S. K. Lin, Recent trends in green and sustainable chemistry:

rethinking textile waste in a circular economy, *Curr. Opin. Green Sustainable Chem.*, 2019, **20**, 1–10.

21 H. T. T. Dang, C. V. Dinh, K. M. Nguyen, N. T. H. Tran, T. T. Pham and R. M. Narbaitz, Loofah sponges as bio-carriers in a pilot-scale integrated fixed-film activated sludge system for municipal wastewater treatment, *Sustainability*, 2020, **12**, 4758.

22 W. Q. Yin, D. Dai, J. H. Hou, S. S. Wang, X. G. Wu and X. Z. Wang, Hierarchical porous biochar-based functional materials derived from biowaste for Pb(II) removal, *Appl. Surf. Sci.*, 2019, **465**, 297–302.

23 J. D. Dai, L. Qin, R. L. Zhang, A. T. Xie, Z. S. Chang, S. J. Tian, C. X. Li and Y. S. Yan, Sustainable bovine bone-derived hierarchically porous carbons with excellent adsorption of antibiotics: Equilibrium, kinetic and thermodynamic investigation, *Powder Technol.*, 2018, **331**, 162–170.

24 J. Li, B. Michalkiewicz, J. Min, C. Ma, X. Chen, J. Gong, E. Mijowska and T. Tang, Selective preparation of biomass-derived porous carbon with controllable pore sizes toward highly efficient CO_2 capture, *Chem. Eng. J.*, 2019, **360**, 250–259.

25 Z. Wang, S. Yun, H. Xu, C. Wang, Y. Zhang, J. Chen and B. Jia, Mesophilic anaerobic co-digestion of acorn slag waste with dairy manure in a batch digester: Focusing on mixing ratios and bio-based carbon accelerants, *Bioresour. Technol.*, 2019, **286**, 121394.

26 N. Varshney, M. Tariq, F. Arshad and M. P. Sk, Biomass-derived carbon dots for efficient cleanup of oil spills, *J. Water Process Eng.*, 2022, **49**, 103016.

27 D. V. Cuong, P.-C. Wu, N.-L. Liu and C.-H. Hou, Hierarchical porous carbon derived from activated biochar as an eco-friendly electrode for the electrosorption of inorganic ions, *Sep. Purif. Technol.*, 2020, **242**, 116813.

28 V. C. Dinh, N. M. Hiep, T. T. H. Hoa, V.-A. Nguyen, C.-H. Hou, C.-S. Fan and N. Van Truc, Development of a capacitive deionization stack with highly porous oxygen-doped carbon electrodes for brackish water desalination in remote coastal areas, *Mater. Chem. Phys.*, 2023, **307**, 128165.

29 Z. Gao, S. Yun, C. Yang, Y. Zhang, J. Dang, G. Yang, T. Yang, D. Qiao and K. Wang, Niobium- and cobalt-modified dual-source-derived porous carbon with a honeycomb-like stable structure for supercapacitor and hydrogen evolution reaction, *J. Colloid Interface Sci.*, 2023, **639**, 33–48.

30 X. Wang, S. Yun, W. Fang, C. Zhang, X. Liang, Z. Lei and Z. Liu, Layer-stacking activated carbon derived from sunflower stalk as electrode materials for high-performance supercapacitors, *ACS Sustainable Chem. Eng.*, 2018, **6**, 11397–11407.

31 Z. Wang, S. Yun, X. Wang, C. Wang, Y. Si, Y. Zhang and H. Xu, Aloe peel-derived honeycomb-like bio-based carbon with controllable morphology and its superior electrochemical properties for new energy devices, *Ceram. Int.*, 2019, **45**, 4208–4218.

32 J. Q. Xu, K. Zhou, F. Chen, W. Chen, X. F. Wei, X. W. Liu and J. H. Liu, Natural integrated carbon architecture for rechargeable lithium-sulfur batteries, *ACS Sustainable Chem. Eng.*, 2016, **4**, 666–670.

33 Z. W. Tian, Y. Qiu, J. C. Zhou, X. B. Zhao and J. J. Cai, The direct carbonization of algae biomass to hierarchical porous carbons and CO_2 adsorption properties, *Mater. Lett.*, 2016, **180**, 162–165.

34 M. Liu, M. Xu, Y. Xue, W. Ni, S. Huo, L. Wu, Z. Yang and Y. Yan, Efficient capacitive deionization using natural basswood derived, free standing, hierarchically porous carbon electrodes, *ACS Appl. Mater. Interfaces*, 2018, **10**, 31260–31270.

35 J. Hou, C. Cao, F. Idrees and X. Ma, Hierarchical porous nitrogen-doped carbon nanosheets derived from silk for ultrahigh-capacity battery anodes and supercapacitors, *ACS Nano*, 2015, **9**, 2556–2564.

36 S. J. Song, F. W. Ma, G. Wu, D. Ma, W. D. Geng and J. F. Wan, Facile self-templating large scale preparation of biomass-derived 3D hierarchical porous carbon for advanced supercapacitors, *J. Mater. Chem. A*, 2015, **3**, 18154–18162.

37 J. Liu, Y. Deng, X. Li and L. Wang, Promising nitrogen-rich porous carbons derived from one-step calcium chloride activation of biomass-based waste for high performance supercapacitors, *ACS Sustainable Chem. Eng.*, 2016, **4**, 177–187.

38 Y. Zhu, G. Y. Xu, X. L. Zhang, S. J. Wang, C. Li and G. X. Wang, Hierarchical porous carbon derived from soybean hulls as a cathode matrix for lithium-sulfur batteries, *J. Alloys Compd.*, 2017, **695**, 2246–2252.

39 Y. Zhao, W. Ran, J. He, Y. Song, C. Zhang, D. B. Xiong, F. Gao, J. Wu and Y. Xia, Oxygen-rich hierarchical porous carbon derived from artemia cyst shells with superior electrochemical performance, *ACS Appl. Mater. Interfaces*, 2015, **7**, 1132–1139.

40 J. T. Sun, J. Niu, M. Y. Liu, J. Ji, M. L. Dou and F. Wang, Biomass-derived nitrogen-doped porous carbons with tailored hierarchical porosity and high specific surface area for high energy and power density supercapacitors, *Appl. Surf. Sci.*, 2018, **427**, 807–813.

41 R. Y. Zhong and B. F. Sels, Sulfonated mesoporous carbon and silica-carbon nanocomposites for biomass conversion, *Appl. Catal., B*, 2018, **236**, 518–545.

42 H. B. Ouyang, Q. Q. Gong, C. Y. Li, J. F. Huang and Z. W. Xu, Porphyra derived hierarchical porous carbon with high graphitization for ultra-stable lithium-ion batteries, *Mater. Lett.*, 2019, **235**, 111–115.

43 M. F. Chen, D. Yu, X. Z. Zheng and X. P. Dong, Biomass based N-doped hierarchical porous carbon nanosheets for all-solid-state supercapacitors, *J. Energy Storage*, 2019, **21**, 105–112.

44 Q. Shi, Y. Wang, X. Zhang, B. Shen, F. Wang and Y. Zhang, Hierarchically porous biochar synthesized with $CaCO_3$ template for efficient Hg_0 adsorption from flue gas, *Fuel Process. Technol.*, 2020, **199**, 106247.

45 Y. Du, H. Chen, X. Xu, C. Wang, F. Zhou, Z. Zeng, W. Zhang and L. Li, Surface modification of biomass derived toluene adsorbent: hierarchically porous characterization and

heteroatom doped effect, *Microporous Mesoporous Mater.*, 2020, **293**, 109831.

46 F. Gao, C. Geng, N. Xiao, J. Y. Qu and J. S. Qiu, Hierarchical porous carbon sheets derived from biomass containing an activation agent and in-built template for lithium ion batteries, *Carbon*, 2018, **139**, 1085–1092.

47 J. Huang, L. Chen, H. Dong, Y. Zeng, H. Hu, M. Zheng, Y. Liu, Y. Xiao and Y. Liang, Hierarchical porous carbon with network morphology derived from natural leaf for superior aqueous symmetrical supercapacitors, *Electrochim. Acta*, 2017, **258**, 504–511.

48 J. Kim, Y. Yi, D. H. Peck, S. H. Yoon, D. H. Jung and H. S. Park, Controlling hierarchical porous structures of rice-husk-derived carbons for improved capacitive deionization performance, *Environ. Sci.: Nano*, 2019, **6**, 916–924.

49 Y. C. Zhang, Y. You, S. Xin, Y. X. Yin, J. Zhang, P. Wang, X. S. Zheng, F. F. Cao and Y. G. Guo, Rice husk-derived hierarchical silicon/nitrogen-doped carbon/carbon nanotube spheres as low-cost and high-capacity anodes for lithium-ion batteries, *Nano Energy*, 2016, **25**, 120–127.

50 M. K. Rybarczyk, H. J. Peng, C. Tang, M. Lieder, Q. Zhang and M. M. Titirici, Porous carbon derived from rice husks as sustainable bioresources: insights into the role of micro-/mesoporous hierarchy in hosting active species for lithium-sulphur batteries, *Green Chem.*, 2016, **18**, 5169–5179.

51 D. V. Cuong, B. M. Matsagar, M. Lee, M. S. A. Hossain, Y. Yamauchi, M. Vithanage, B. Sarkar, Y. S. Ok, K. C. W. Wu and C.-H. Hou, A critical review on biochar-based engineered hierarchical porous carbon for capacitive charge storage, *Renewable Sustainable Energy Rev.*, 2021, **145**, 111029.

52 J. Zhang, N. Zhang, F. M. Tack, S. Sato, D. S. Alessi, P. Oleszczuk, H. Wang, X. Wang and S. Wang, Modification of ordered mesoporous carbon for removal of environmental contaminants from aqueous phase: A review, *J. Hazard. Mater.*, 2021, 126266.

53 J. Mu, S. I. Wong, Q. Li, P. Zhou, J. Zhou, Y. Zhao, J. Sunarso and S. Zhuo, Fishbone-derived N-doped hierarchical porous carbon as an electrode material for supercapacitor, *J. Alloys Compd.*, 2020, **832**, 154950.

54 J. Wang, P. Zhang, L. Liu, Y. Zhang, J. Yang, Z. Zeng and S. Deng, Controllable synthesis of bifunctional porous carbon for efficient gas-mixture separation and high-performance supercapacitor, *Chem. Eng. J.*, 2018, **348**, 57–66.

55 B. Chang, W. Shi, H. Yin, S. Zhang and B. Yang, Poplar catkin-derived self-templated synthesis of N-doped hierarchical porous carbon microtubes for effective CO_2 capture, *Chem. Eng. J.*, 2019, **358**, 1507–1518.

56 S. Chen, J. Wang, Z. Wu, Q. Deng, W. Tu, G. Dai, Z. Zeng and S. Deng, Enhanced Cr(VI) removal by polyethylenimine- and phosphorus-codoped hierarchical porous carbons, *J. Colloid Interface Sci.*, 2018, **523**, 110–120.

57 L. Qin, Z. P. Zhou, J. D. Dai, P. Ma, H. B. Zhao, J. S. He, A. Xie, C. X. Li and Y. S. Yan, Novel N-doped hierarchically porous carbons derived from sustainable shrimp shell for high-performance removal of sulfamethazine and chloramphenicol, *J. Taiwan Inst. Chem. Eng.*, 2016, **62**, 228–238.

58 J. Sun, M. Li, Z. Zhang and J. Guo, Unravelling the adsorption disparity mechanism of heavy-metal ions on the biomass-derived hierarchically porous carbon, *Appl. Surf. Sci.*, 2019, **471**, 615–620.

59 W. Zhang, Y. Bao and A. Bao, Preparation of nitrogen-doped hierarchical porous carbon materials by a template-free method and application to CO_2 capture, *J. Environ. Chem. Eng.*, 2020, **8**, 103732.

60 F. Liu, Y. Zhang, P. Zhang, M. Xu, T. Tan, J. Wang, Q. Deng, L. Zhang, Y. Wan and S. Deng, Facile preparation of N and O-rich porous carbon from palm sheath for highly selective separation of $CO_2/CH_4/N_2$ gas-mixture, *Chem. Eng. J.*, 2020, **399**, 125812.

61 Y. Wang, Y. Gu, H. Li, M. Ye, W. Qin, H. Zhang, G. Wang, Y. Zhang and H. Zhao, Electrodeposition of hierarchically amorphous FeOOH nanosheets on carbonized bamboo as an efficient filter membrane for As(III) removal, *Chem. Eng. J.*, 2020, **392**, 123773.

62 H. Zhou, B. Yan, J. Lai, H. Liu, A. Ma, W. Chen, X. Jin, W. Zhao and G. Zhang, Renewable biomass derived hierarchically porous carbonaceous sponges and their magnetic nanocomposites for removal of organic molecules from water, *J. Ind. Eng. Chem.*, 2018, **58**, 334–342.

63 K. Zhou, W. Ma, Z. Zeng, R. chen, X. Xu, B. Liu, H. Li, H. Li and L. Li, Waste biomass-derived oxygen and nitrogen co-doped porous carbon/MgO composites as superior acetone adsorbent: Experimental and DFT study on the adsorption behavior, *Chem. Eng. J.*, 2020, **387**, 124173.

64 Y. Bing, H. Liu, L. Zhang, D. Ghosh and J. Zhang, Nanostructured Pt-alloy electrocatalysts for PEM fuel cell oxygen reduction reaction, *Chem. Soc. Rev.*, 2010, **39**, 2184–2202.

65 C. Hu, Y. Xiao, Y. Zou and L. Dai, Carbon-based metal-free electrocatalysis for energy conversion, energy storage, and environmental protection, *Electrochem. Energy Rev.*, 2018, **1**, 84–112.

66 D. Tu, H. Liao, Q. Deng, X. Liu, R. Shang and X. Zhang, Renewable biomass derived porous BCN nanosheets and their adsorption and photocatalytic activities for the decontamination of organic pollutants, *RSC Adv.*, 2018, **8**, 21905–21914.

67 X. Yang, Z. Chen, W. Zhao, C. Liu, X. Qian, M. Zhang, G. Wei, E. Khan, Y. H. Ng and Y. S. Ok, Recent advances in photodegradation of antibiotic residues in Water, *Chem. Eng. J.*, 2020, 126806.

68 J. C. Colmenares, R. S. Varma and P. Lisowski, Sustainable hybrid photocatalysts: titania immobilized on carbon materials derived from renewable and biodegradable resources, *Green Chem.*, 2016, **18**, 5736–5750.

69 Z. Sun, X. Wu, K. Qu, Z. Huang, S. Liu, M. Dong and Z. Guo, Bimetallic metal-organic frameworks anchored corncob-derived porous carbon photocatalysts for synergistic

degradation of organic pollutants, *Chemosphere*, 2020, **259**, 127389.

70 J. Hu, L. Zhang, B. Lu, X. Wang and H. Huang, $LaMnO_3$ nanoparticles supported on N doped porous carbon as efficient photocatalyst, *Vacuum*, 2019, **159**, 59–68.

71 M. Shi, W. Wei, Z. Jiang, H. Han, J. Gao and J. Xie, Biomass-derived multifunctional TiO_2/carbonaceous aerogel composite as a highly efficient photocatalyst, *RSC Adv.*, 2016, **6**, 25255–25266.

72 R. Djellabi, B. Yang, Y. Wang, X. Cui and X. Zhao, Carbonaceous biomass-titania composites with TiOC bonding bridge for efficient photocatalytic reduction of Cr(VI) under narrow visible light, *Chem. Eng. J.*, 2019, **366**, 172–180.

73 X. Hu, Y. Deng, J. Zhou, B. Liu, A. Yang, T. Jin and Y. F. Tsang, N-and O self-doped biomass porous carbon cathode in an electro-Fenton system for Chloramphenicol degradation, *Sep. Purif. Technol.*, 2020, **251**, 117376.

74 P. Lisowski, J. C. Colmenares, O. Mašek, W. Lisowski, D. Lisovytskiy, A. Kamińska and D. Łomot, Dual functionality of TiO_2/biochar hybrid materials: photocatalytic phenol degradation in the liquid phase and selective oxidation of methanol in the gas phase, *ACS Sustainable Chem. Eng.*, 2017, **5**, 6274–6287.

75 Y. Zhou, T. Cai, S. Liu, Y. Liu, H. Chen, Z. Li, J. Du, Z. Lei and H. Peng, N-doped magnetic three-dimensional carbon microspheres@TiO_2 with a porous architecture for enhanced degradation of tetracycline and methyl orange *via* adsorption/photocatalysis synergy, *Chem. Eng. J.*, 2021, **411**, 128615.

76 J. R. de Andrade, M. G. A. Vieira, M. G. C. da Silva and S. Wang, Oxidative degradation of pharmaceutical losartan potassium with N-doped hierarchical porous carbon and peroxymonosulfate, *Chem. Eng. J.*, 2020, **382**, 122971.

77 H. Fu, S. Ma, P. Zhao, S. Xu and S. Zhan, Activation of peroxymonosulfate by graphitized hierarchical porous biochar and $MnFe_2O_4$ magnetic nanoarchitecture for organic pollutants degradation: Structure dependence and mechanism, *Chem. Eng. J.*, 2019, **360**, 157–170.

78 M. Xie, J. Tang, G. Fang, M. Zhang, L. Kong, F. Zhu, L. Ma, D. Zhou and J. Zhan, Biomass Schiff base polymer-derived N-doped porous carbon embedded with CoO nanodots for adsorption and catalytic degradation of chlorophenol by peroxymonosulfate, *J. Hazard. Mater.*, 2020, **384**, 121345.

79 R. J. Nicholls, A. T. Murdock, J. Tsang, J. Britton, T. J. Pennycook, A. Koós, P. D. Nellist, N. Grobert and J. R. Yates, Probing the bonding in nitrogen-doped graphene using electron energy loss spectroscopy, *ACS Nano*, 2013, **7**, 7145–7150.

80 X. Chen, W.-D. Oh, Z.-T. Hu, Y.-M. Sun, R. D. Webster, S.-Z. Li and T.-T. Lim, Enhancing sulfacetamide degradation by peroxymonosulfate activation with N-doped graphene produced through delicately-controlled nitrogen functionalization *via* tweaking thermal annealing processes, *Appl. Catal., B*, 2018, **225**, 243–257.

81 Y. Yao, C. Lian, G. Wu, Y. Hu, F. Wei, M. Yu and S. Wang, Synthesis of "sea urchin"-like carbon nanotubes/porous carbon superstructures derived from waste biomass for treatment of various contaminants, *Appl. Catal., B*, 2017, **219**, 563–571.

82 W. Ma, N. Wang, Y. Du, P. Xu, B. Sun, L. Zhang and K.-Y. A. Lin, Human-hair-derived N, S-doped porous carbon: an enrichment and degradation system for wastewater remediation in the presence of peroxymonosulfate, *ACS Sustainable Chem. Eng.*, 2018, **7**, 2718–2727.

83 J. Liu, Z. Zhao, P. Shao and F. Cui, Activation of peroxymonosulfate with magnetic Fe_3O_4–MnO_2 core–shell nanocomposites for 4-chlorophenol degradation, *Chem. Eng. J.*, 2015, **262**, 854–861.

84 S. Yang, X. Qiu, P. Jin, M. Dzakpasu, X. C. Wang, Q. Zhang, L. Yang, D. Ding, W. Wang and K. Wu, MOF-templated synthesis of $CoFe_2O_4$ nanocrystals and its coupling with peroxymonosulfate for degradation of bisphenol A, *Chem. Eng. J.*, 2018, **353**, 329–339.

85 N. Singh and B. R. Goldsmith, Role of electrocatalysis in the remediation of water pollutants, *ACS Catal.*, 2020, **10**, 3365–3371.

86 P. S. Patel, N. Bandre, A. Saraf and J. P. Ruparelia, Electro-catalytic materials (electrode materials) in electrochemical wastewater treatment, *Procedia Eng.*, 2013, **51**, 430–435.

87 M. Tian, Y. Zhu, D. Zhang, M. Wang, Y. Chen, Y. Yang and S. Gao, Pyrrolic-nitrogen-rich biomass-derived catalyst for sustainable degradation of organic pollutant *via* a self-powered electro-Fenton process, *Nano Energy*, 2019, **64**, 103940.

88 Y. Chen, Y. Zhu, M. Tian, C. Chen, X. Jia and S. Gao, Sustainable self-powered electro-Fenton degradation of organic pollutants in wastewater using carbon catalyst with controllable pore activated by EDTA-2Na, *Nano Energy*, 2019, **59**, 346–353.

89 P. Zhou, J. Wan, X. Wang, J. Chen, Y. Gong and K. Xu, Three-dimensional hierarchical porous carbon cathode derived from waste tea leaves for the electrocatalytic degradation of phenol, *Langmuir*, 2019, **35**, 12914–12926.

90 Y. Gong, J. Wan, P. Zhou, X. Wang, J. Chen and K. Xu, Oxygen and nitrogen-enriched hierarchical MoS_2 nanospheres decorated cornstalk-derived activated carbon for electrocatalytic degradation and supercapacitors, *Mater. Sci. Semicond. Process.*, 2020, 105533.

91 E. Brillas, I. Sirés and M. A. Oturan, Electro-Fenton process and related electrochemical technologies based on Fenton's reaction chemistry, *Chem. Rev.*, 2009, **109**, 6570–6631.

92 Y. Yang, F. He, Y. Shen, X. Chen, H. Mei, S. Liu and Y. Zhang, A biomass derived N/C-catalyst for the electrochemical production of hydrogen peroxide, *Chem. Commun.*, 2017, **53**, 9994–9997.

93 K. Zhao, X. Quan, S. Chen, H. Yu, Y. Zhang and H. Zhao, Enhanced electro-Fenton performance by fluorine-doped porous carbon for removal of organic pollutants in wastewater, *Chem. Eng. J.*, 2018, **354**, 606–615.

94 M. Arora, B. Kiran, S. Rani, A. Rani, B. Kaur and N. Mittal, Heavy metal accumulation in vegetables irrigated with water from different sources, *Food Chem.*, 2008, **111**, 811–815.

95 A. Demirbas, Heavy metal adsorption onto agro-based waste materials: A review, *J. Hazard. Mater.*, 2008, **157**, 220–229.

96 Y. Yu, C. Zhang, L. Yang and J. Paul Chen, Cerium oxide modified activated carbon as an efficient and effective adsorbent for rapid uptake of arsenate and arsenite: Material development and study of performance and mechanisms, *Chem. Eng. J.*, 2017, **315**, 630–638.

97 Y. Yin, T. Zhou, H. Luo, J. Geng, W. Yu and Z. Jiang, Adsorption of arsenic by activated charcoal coated zirconium-manganese nanocomposite: Performance and mechanism, *Colloids Surf., A*, 2019, **575**, 318–328.

98 Y. Xiong, Q. Tong, W. Shan, Z. Xing, Y. Wang, S. Wen and Z. Lou, Arsenic transformation and adsorption by iron hydroxide/manganese dioxide doped straw activated carbon, *Appl. Surf. Sci.*, 2017, **416**, 618–627.

99 A. Kumar and H. M. Jena, Adsorption of Cr(VI) from aqueous phase by high surface area activated carbon prepared by chemical activation with $ZnCl_2$, *Process Saf. Environ. Prot.*, 2017, **109**, 63–71.

100 I. Enniya, L. Rghioui and A. Jourani, Adsorption of hexavalent chromium in aqueous solution on activated carbon prepared from apple peels, *Sustainable Chem. Pharm.*, 2018, **7**, 9–16.

101 W. Qiu, D. Yang, J. Xu, B. Hong, H. Jin, D. Jin, X. Peng, J. Li, H. Ge and X. Wang, Efficient removal of Cr(VI) by magnetically separable $CoFe_2O_4$/activated carbon composite, *J. Alloys Compd.*, 2016, **678**, 179–184.

102 E. Asuquo, A. Martin, P. Nzerem, F. Siperstein and X. Fan, Adsorption of Cd(II) and Pb(II) ions from aqueous solutions using mesoporous activated carbon adsorbent: Equilibrium, kinetics and characterisation studies, *J. Environ. Chem. Eng.*, 2017, **5**, 679–698.

103 D. Lv, Y. Liu, J. Zhou, K. Yang, Z. Lou, S. A. Baig and X. Xu, Application of EDTA-functionalized bamboo activated carbon (BAC) for Pb(II) and Cu(II) removal from aqueous solutions, *Appl. Surf. Sci.*, 2018, **428**, 648–658.

104 X. Liu, D. Lai and Y. Wang, Performance of Pb(II) removal by an activated carbon supported nanoscale zero-valent iron composite at ultralow iron content, *J. Hazard. Mater.*, 2019, **361**, 37–48.

105 Q. Zia, M. Tabassum, Z. Lu, M. T. Khawar, J. Song, H. Gong, J. Meng, Z. Li and J. Li, Porous poly(L-lactic acid)/chitosan nanofibres for copper ion adsorption, *Carbohydr. Polym.*, 2020, **227**, 115343.

106 S. Zhuang and J. Wang, Removal of cobalt ion from aqueous solution using magnetic graphene oxide/chitosan composite, *Environ. Prog. Sustainable Energy*, 2019, **38**, S32–S41.

107 A. L. P. Xavier, O. F. H. Adarme, L. M. Furtado, G. M. D. Ferreira, L. H. M. da Silva, L. F. Gil and L. V. A. Gurgel, Modeling adsorption of copper(II), cobalt(II) and nickel(II) metal ions from aqueous solution onto a new carboxylated sugarcane bagasse. Part II: Optimization of monocomponent fixed-bed column adsorption, *J. Colloid Interface Sci.*, 2018, **516**, 431–445.

108 J. T. Sun, Z. P. Zhang, J. Ji, M. L. Dou and F. Wang, Removal of Cr^{6+} from wastewater *via* adsorption with high-specific-surface-area nitrogen-doped hierarchical porous carbon derived from silkworm cocoon, *Appl. Surf. Sci.*, 2017, **405**, 372–379.

109 Y. Li, M. Xu, H. Yin, W. Shi, G. I. N. Waterhouse, H. Li and S. Ai, Yolk-shell Fe_3O_4 nanoparticles loaded on persimmon-derived porous carbon for supercapacitor assembly and As(V) removal, *J. Alloys Compd.*, 2019, **810**, 151887.

110 W. Tian, H. Zhang, X. Duan, H. Sun, M. O. Tade, H. M. Ang and S. Wang, Nitrogen- and sulfur-codoped hierarchically porous carbon for adsorptive and oxidative removal of pharmaceutical contaminants, *ACS Appl. Mater. Interfaces*, 2016, **8**, 7184–7193.

111 A. B. Albadarin, M. N. Collins, M. Naushad, S. Shirazian, G. Walker and C. Mangwandi, Activated lignin-chitosan extruded blends for efficient adsorption of methylene blue, *Chem. Eng. J.*, 2017, **307**, 264–272.

112 D. S. Tong, C. W. Wu, M. O. Adebajo, G. C. Jin, W. H. Yu, S. F. Ji and C. H. Zhou, Adsorption of methylene blue from aqueous solution onto porous cellulose-derived carbon/montmorillonite nanocomposites, *Appl. Clay Sci.*, 2018, **161**, 256–264.

113 J. Zhang, X. Yan, X. Hu, R. Feng and M. Zhou, Direct carbonization of Zn/Co zeolitic imidazolate frameworks for efficient adsorption of Rhodamine B, *Chem. Eng. J.*, 2018, **347**, 640–647.

114 Z. Li, X. Meng and Z. Zhang, Equilibrium and kinetic modelling of adsorption of Rhodamine B on MoS_2, *Mater. Res. Bull.*, 2019, **111**, 238–244.

115 S. Zhuang, R. Chen, Y. Liu and J. Wang, Magnetic COFs for the adsorptive removal of diclofenac and sulfamethazine from aqueous solution: Adsorption kinetics, isotherms study and DFT calculation, *J. Hazard. Mater.*, 2020, **385**, 121596.

116 Z. Chang, J. Dai, A. Xie, J. He, R. Zhang, S. Tian, Y. Yan, C. Li, W. Xu and R. Shao, From lignin to three-dimensional interconnected hierarchically porous carbon with high surface area for fast and superhigh-efficiency adsorption of sulfamethazine, *Ind. Eng. Chem. Res.*, 2017, **56**, 9367–9375.

117 J. Dai, S. Tian, Y. Jiang, Z. Chang, A. Xie, R. Zhang, C. Li and Y. Yan, Fe_3C/Fe/C magnetic hierarchical porous carbon with micromesopores for highly efficient chloramphenicol adsorption: Magnetization, graphitization, and adsorption properties investigation, *Ind. Eng. Chem. Res.*, 2018, **57**, 3510–3522.

118 J. Lach, Adsorption of chloramphenicol on commercial and modified activated carbons, *Water*, 2019, **11**, 1141.

119 C. Zhang, W. Zhang, M. Yu, K. Ning, L. Zhang, X. Wang and X. He, Synthesis of hollow porous carbon nanospheres from coal tar for adsorption of Direct Black 38 dye, *J. Porous Mater.*, 2017, **24**, 1289–1293.

120 X. Yang, H. Yi, X. Tang, S. Zhao, Z. Yang, Y. Ma, T. Feng and X. Cui, Behaviors and kinetics of toluene adsorption-desorption on activated carbons with varying pore structure, *J. Environ. Sci.*, 2018, **67**, 104–114.

121 Y. Shen and N. Zhang, Facile synthesis of porous carbons from silica-rich rice husk char for volatile organic compounds (VOCs) sorption, *Bioresour. Technol.*, 2019, **282**, 294–300.

122 J. Cheng, J.-J. Gu, W. Tao, P. Wang, L. Liu, C.-Y. Wang, Y.-K. Li, X.-H. Feng, G.-H. Qiu and F.-F. Cao, Edible fungus slag derived nitrogen-doped hierarchical porous carbon as a high-performance adsorbent for rapid removal of organic pollutants from water, *Bioresour. Technol.*, 2019, **294**, 122149.

123 L. Chen, T. Ji, L. Mu, Y. Shi, H. Wang and J. Zhu, Pore size dependent molecular adsorption of cationic dye in biomass derived hierarchically porous carbon, *J. Environ. Manage.*, 2017, **196**, 168–177.

124 X. Wei, Z. D. Zhang, L. Qin and J. D. Dai, Template-free preparation of yeast-derived three-dimensional hierarchical porous carbon for highly efficient sulfamethazine adsorption from water, *J. Taiwan Inst. Chem. Eng.*, 2019, **95**, 532–540.

125 M. Tang, X. Huang, Y. Peng and S. Lu, Hierarchical porous carbon as a highly efficient adsorbent for toluene and benzene, *Fuel*, 2020, **270**, 117478.

126 X. Ge, Y. Ma, X. Song, G. Wang, H. Zhang, Y. Zhang and H. Zhao, β-FeOOH nanorods/carbon foam-based hierarchically porous monolith for highly effective arsenic removal, *ACS Appl. Mater. Interfaces*, 2017, **9**, 13480–13490.

127 X. Ge, D. Xie and Y. Zhang, A 3D porous carbon foam loaded with Fe_3O_4/graphene oxide for highly effective As(III) removal, *New J. Chem.*, 2020, **44**, 12926–12931.

128 A. U. Rajapaksha, M. S. Alam, N. Chen, D. S. Alessi, A. D. Igalavithana, D. C. W. Tsang and Y. S. Ok, Removal of hexavalent chromium in aqueous solutions using biochar: Chemical and spectroscopic investigations, *Sci. Total Environ.*, 2018, **625**, 1567–1573.

129 S. Mandal, B. Sarkar, N. Bolan, Y. S. Ok and R. Naidu, Enhancement of chromate reduction in soils by surface modified biochar, *J. Environ. Manage.*, 2017, **186**, 277–284.

130 C. T. Hsieh and H. S. Teng, Influence of mesopore volume and adsorbate size on adsorption capacities of activated carbons in aqueous solutions, *Carbon*, 2000, **38**, 863–869.

131 X. Zhuang, Y. Wan, C. M. Feng, Y. Shen and D. Y. Zhao, Highly efficient adsorption of bulky dye molecules in wastewater on ordered mesoporous carbons, *Chem. Mater.*, 2009, **21**, 706–716.

132 Y. Zhang, G. Ji, C. Li, X. Wang and A. Li, Templating synthesis of hierarchical porous carbon from heavy residue of tire pyrolysis oil for methylene blue removal, *Chem. Eng. J.*, 2020, **390**, 124398.

133 D. V. Cuong and C.-H. Hou, Engineered biochar prepared using a self-template coupled with physicochemical activation for highly efficient adsorption of crystal violet, *J. Taiwan Inst. Chem. Eng.*, 2022, **139**, 104533.

134 C. A. Trickett, A. Helal, B. A. Al-Maythalony, Z. H. Yamani, K. E. Cordova and O. M. Yaghi, The chemistry of metal–organic frameworks for CO_2 capture, regeneration and conversion, *Nat. Rev. Mater.*, 2017, **2**, 17045.

135 P. D. Dissanayake, S. You, A. D. Igalavithana, Y. Xia, A. Bhatnagar, S. Gupta, H. W. Kua, S. Kim, J.-H. Kwon, D. C. W. Tsang and Y. S. Ok, Biochar-based adsorbents for carbon dioxide capture: A critical review, *Renewable Sustainable Energy Rev.*, 2020, **119**, 109582.

136 A. E. Creamer and B. Gao, Carbon-based adsorbents for postcombustion CO_2 capture: a critical review, *Environ. Sci. Technol.*, 2016, **50**, 7276–7289.

137 P. D. Dissanayake, S. W. Choi, A. D. Igalavithana, X. Yang, D. C. W. Tsang, C.-H. Wang, H. W. Kua, K. B. Lee and Y. S. Ok, Sustainable gasification biochar as a high efficiency adsorbent for CO_2 capture: A facile method to designer biochar fabrication, *Renewable Sustainable Energy Rev.*, 2020, **124**, 109785.

138 A. D. Igalavithana, S. W. Choi, P. D. Dissanayake, J. Shang, C.-H. Wang, X. Yang, S. Kim, D. C. W. Tsang, K. B. Lee and Y. S. Ok, Gasification biochar from biowaste (food waste and wood waste) for effective CO_2 adsorption, *J. Hazard. Mater.*, 2020, **391**, 121147.

139 A. Gao, N. Guo, M. Yan, M. Li, F. Wang and R. Yang, Hierarchical porous carbon activated by $CaCO_3$ from pigskin collagen for CO_2 and H_2 adsorption, *Microporous Mesoporous Mater.*, 2018, **260**, 172–179.

140 X. Liu, C. Sun, H. Liu, W. H. Tan, W. Wang and C. Snape, Developing hierarchically ultra-micro/mesoporous biocarbons for highly selective carbon dioxide adsorption, *Chem. Eng. J.*, 2019, **361**, 199–208.

141 H. Sun, B. Yang and A. Li, Biomass derived porous carbon for efficient capture of carbon dioxide, organic contaminants and volatile iodine with exceptionally high uptake, *Chem. Eng. J.*, 2019, **372**, 65–73.

142 H. M. Wei, J. Chen, N. Fu, H. J. Chen, H. L. Lin and S. Han, Biomass-derived nitrogen-doped porous carbon with superior capacitive performance and high CO_2 capture capacity, *Electrochim. Acta*, 2018, **266**, 161–169.

143 B. Liu, W. Wang, N. Wang and C. T. Au, Preparation of activated carbon with high surface area for high-capacity methane storage, *J. Energy Chem.*, 2014, **23**, 662–668.

144 D. Qian, C. Lei, G.-P. Hao, W.-C. Li and A.-H. Lu, Synthesis of hierarchical porous carbon monoliths with incorporated metal–organic frameworks for enhancing volumetric based CO_2 capture capability, *ACS Appl. Mater. Interfaces*, 2012, **4**, 6125–6132.

145 W. Chen, X. Wang, Z. Hashisho, M. Feizbakhshan, P. Shariaty, S. Niknaddaf and X. Zhou, Template-free and fast one-step synthesis from enzymatic hydrolysis lignin to hierarchical porous carbon for CO_2 capture, *Microporous Mesoporous Mater.*, 2019, **280**, 57–65.

146 C. Chen, H. Huang, Y. Yu, J. Shi, C. He, R. Albilali and H. Pan, Template-free synthesis of hierarchical porous carbon with controlled morphology for CO_2 efficient capture, *Chem. Eng. J.*, 2018, **353**, 584–594.

147 W. Kong, Y. Liu and J. Liu, Design of highly nitrogen-doped, two-dimensional hierarchical porous carbons with superior performance for selective capture of CO_2 and SO_2, *Energy Fuels*, 2020, **34**, 3557–3565.
148 B. Ding, X. Wang, Y. Xu, S. Feng, Y. Ding, Y. Pan, W. Xu and H. Wang, Hydrothermal preparation of hierarchical ZIF-L nanostructures for enhanced CO_2 capture, *J. Colloid Interface Sci.*, 2018, **519**, 38–43.
149 S. Gu, J. He, Y. Zhu, Z. Wang, D. Chen, G. Yu, C. Pan, J. Guan and K. Tao, Facile carbonization of microporous organic polymers into hierarchically porous carbons targeted for effective CO_2 uptake at low pressures, *ACS Appl. Mater. Interfaces*, 2016, **8**, 18383–18392.
150 C. Lu, H. Bai, B. Wu, F. Su and J. F. Hwang, Comparative study of CO_2 capture by carbon nanotubes, activated carbons, and zeolites, *Energy Fuels*, 2008, **22**, 3050–3056.
151 X. Ma, L. Li, R. Chen, C. Wang, H. Li and S. Wang, Heteroatom-doped nanoporous carbon derived from MOF-5 for CO_2 capture, *Appl. Surf. Sci.*, 2018, **435**, 494–502.
152 G. P. Hao, W. C. Li, D. Qian and A. H. Lu, Rapid synthesis of nitrogen-doped porous carbon monolith for CO_2 capture, *Adv. Mater.*, 2010, **22**, 853–857.
153 X. Zhang, S. H. Zhang, H. P. Yang, Y. Feng, Y. Q. Chen, X. H. Wang and H. P. Chen, Nitrogen enriched biochar modified by high temperature CO_2-ammonia treatment: Characterization and adsorption of CO_2, *Chem. Eng. J.*, 2014, **257**, 20–27.
154 H. Zhang, Z. Wang, X. Luo, J. Lu, S. Peng, Y. Wang and L. Han, Constructing hierarchical porous carbons with interconnected micro-mesopores for enhanced CO(2) adsorption, *Front. Chem.*, 2020, **7**, 919.
155 Y. Abbas, S. Yun, Z. Wang, Y. Zhang, X. Zhang and K. Wang, Recent advances in bio-based carbon materials for anaerobic digestion: A review, *Renewable Sustainable Energy Rev.*, 2021, **135**, 110378.
156 T. Xing, S. Yun, B. Li, K. Wang, J. Chen, B. Jia, T. Ke and J. An, Coconut-shell-derived bio-based carbon enhanced microbial electrolysis cells for upgrading anaerobic co-digestion of cow manure and aloe peel waste, *Bioresour. Technol.*, 2021, **338**, 125520.
157 C. Wang, S. Yun, H. Xu, Z. Wang, F. Han, Y. Zhang, Y. Si and M. Sun, Dual functional application of pomelo peel-derived bio-based carbon with controllable morphologies: An efficient catalyst for triiodide reduction and accelerant for anaerobic digestion, *Ceram. Int.*, 2020, **46**, 3292–3303.
158 B. Li, S. Yun, T. Xing, K. Wang, T. Ke and J. An, A strategy for understanding the enhanced anaerobic co-digestion *via* dual-heteroatom doped bio-based carbon and its functional groups, *Chem. Eng. J.*, 2021, **425**, 130473.
159 H. E. Karahan, M. Ji, J. L. Pinilla, X. Han, A. Mohamed, L. Wang, Y. Wang, S. Zhai, A. Montoya and H. Beyenal, Biomass-derived nanocarbon materials for biological applications: challenges and prospects, *J. Mater. Chem. B*, 2020, **8**, 9668–9678.
160 Z. Wang, L. Sheng, X. Yang, J. Sun, Y. Ye, S. Geng, D. Ning, J. Zheng, M. Fan, Y. Zhang and X. Sun, Natural biomass-derived carbon dots as potent antimicrobial agents against multidrug-resistant bacteria and their biofilms, *Sustainable Mater. Technol.*, 2023, **36**, e00584.
161 R. B. Pricilla, M. Maruthapandi, A. Durairaj, I. Kuritka, J. H. T. Luong and A. Gedanken, Biomass-derived Carbon dots and their coated surface as a potential antimicrobial agent, *Biomass Convers. Biorefin.*, 2023, **313**, 137390.
162 T. B. Devi, D. Mohanta and M. Ahmaruzzaman, Biomass derived activated carbon loaded silver nanoparticles: An effective nanocomposites for enhanced solar photocatalysis and antimicrobial activities, *J. Ind. Eng. Chem.*, 2019, **76**, 160–172.
163 T. Chen, M. Li, L. Zhou, X. Ding, D. Lin, T. Duan, G. Yang, R. He and W. Zhu, Bio-inspired biomass-derived carbon aerogels with superior mechanical property for oil–water separation, *ACS Sustainable Chem. Eng.*, 2020, **8**, 6458–6465.
164 S. Gao, X. Li, L. Li and X. Wei, A versatile biomass derived carbon material for oxygen reduction reaction, supercapacitors and oil/water separation, *Nano Energy*, 2017, **33**, 334–342.
165 M. Xu, S. Ma, J. Li, M. Yuan, J. Gao, J. Xue and M. Wang, Multifunctional 3D polydimethylsiloxane modified MoS_2@biomass-derived carbon composite for oil/water separation and organic dye adsorption/photocatalysis, *Colloids Surf., A*, 2022, **637**, 128281.